Chapter 9

Crystal Structures of Organic Compounds

Nader Noroozi Pesyan

Additional information is available at the end of the chapter

http://dx.doi.org/10.5772/48536

1. Introduction

X-ray crystallography is an important method for determination of the arrangement of atoms within a crystal of compound in which a beam of X-rays strikes a crystal and causes the beam of light to spread into many specific directions. From electron density, in the molecule the mean positions of the atoms in the crystal can be determined, as well as their chemical bonds and various other information.

The hexamethylenetetramine as an organic compound was solved in 1923 "(Dickinson & Raymond, 1923)". Several studies of long-chain fatty acids were followed which are an important component of biological membranes "(Bragg, 1925; de Broglie & Trillat, 1925; Caspari, 1928; Müller, 1923, 1928, 1929; Piper, 1929; Saville & Shearer, 1925; Trillat, 1926)". In the 1930s, the structures of larger molecules with two-dimensional complexity began to be solved. An important advance was the structure of phthalocyanine "(Robertson, 1936)", that is closely related to porphyrin molecules important in biology, such as heme, corrin, chlorophyll and etc.

2. Crystal structures of organic compounds

In this chapter, crystal structures of some organic compounds such as organic torsion helicoids, organic compounds consists of intra- and intermolecular hydrogen bond and their some metal complexes and crystal structures of some organic spiro compounds were described.

2.1. Crystal structure of organic torsion helicoids

In recent years, several different interesting organic compounds structures have been found by X-ray crystallography. Helicenes are an extremely attractive and interesting class of conjugated molecules currently investigated for optoelectronic applications "(Groen et al., 1971; Katz, 2000; Rajca et al., 2007; Schmuck, 2003; Urbano, 2003)". They combine the electronic properties afforded by their conjugated system with the chiroptical properties "(Bossi et al., 2009; Collins

& Vachon, 2006; Larsen et al., 1996)" afforded by their interesting and peculiar helix-like structure, resulting from the condensation of aromatic (and/or heteroaromatic) rings, all of them in *ortho* position. For example, the formula and crystal structures of tetrathia-[7]-helicene **1** are shown in Figures 1 and 2, respectively. The compound **1** has been synthesized in three step by starting material of benzo[1,2-*b*:4,3-*b*']dithiophene and is shown in Scheme 1 "(Maiorana et al., 2003)" and this compound showed second-order non-linear optical (NLO) properties and has been investigated (Clays et al., 2003). In particular, carbohelicenes only include benzene rings, and also in heterohelicenes one or more aromatic rings are heterocyclic (pyridine, thiophene, pyrrole and etc.) "(Miyasaka et al., 2005; Rajca et al., 2004)". With increasing number of condensed rings (typically, $n > 4$), the steric interference of the terminal rings forces the molecule to be a helicoidal form. For $n > 4$ the energetic barrier is such that the two enantiomers can be separated and stored "(Martin, 1974; Newman, et al., 1955, 1967; Newman & Lednicer, 1956; Newman & Chen, 1972)". Of course, the conjugation of π system decreases with decreasing of planarity; however, in longer helicenes π-stack interactions can also take place between overlapping rings "(Caronna et al., 2001; Liberko et al., 1993)". All helicenes (generally, $n > 4$) are chiral molecules and exhibit huge specific optical rotations "(Nuckolls et al., 1996, 1998)" since the chromophore itself, in this case the entire aromatic molecule, is inherently dissymmetric (right-hand or left-hand helix), having a twofold symmetry axis, C_2, perpendicular to its cylindrical helix (in carbohelicenes), or inherently asymmetric (in heterohelicenes) "(Wynberg, 1971)".

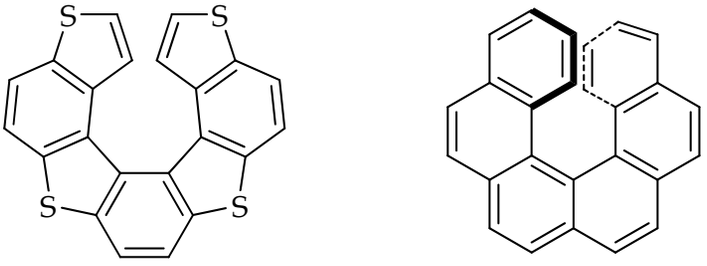

1 **2**

Figure 1. Formula structures of **1** and **2**.

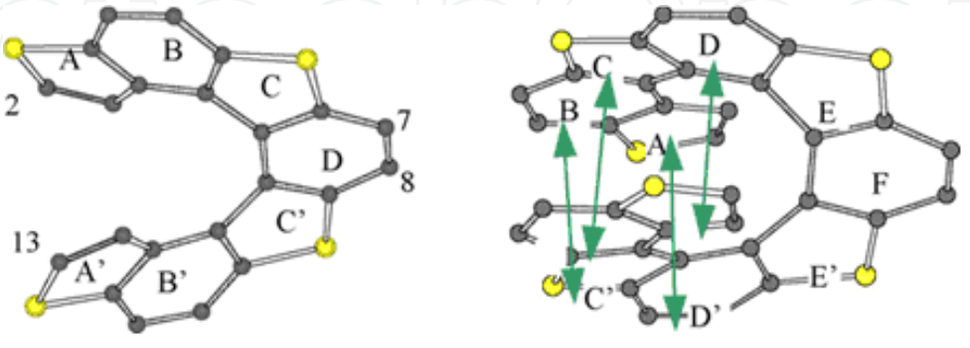

1 ***3***

Figure 2. The helicoid structures of unsubstituted tetrathia-[7]-helicene **1** and unsubstituted hexathia-[11]-helicene **3** "(Caronna et al., 2001)" with the labelling scheme adopted for structural discussion "(Bossi et al., 2009)".

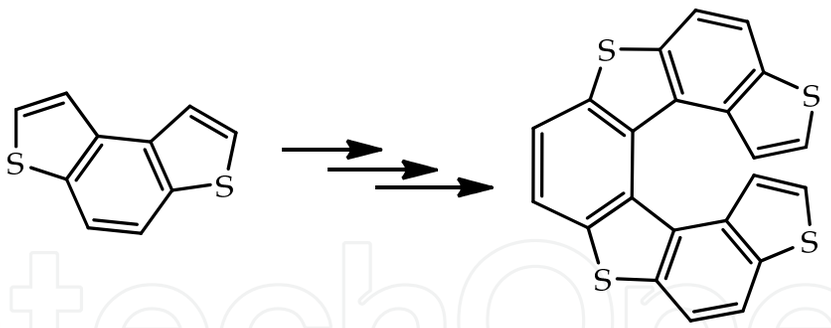

1

Scheme 1. The synthesis of **1** from benzo[1,2-*b*:4,3-*b*']dithiophene as a starting material.

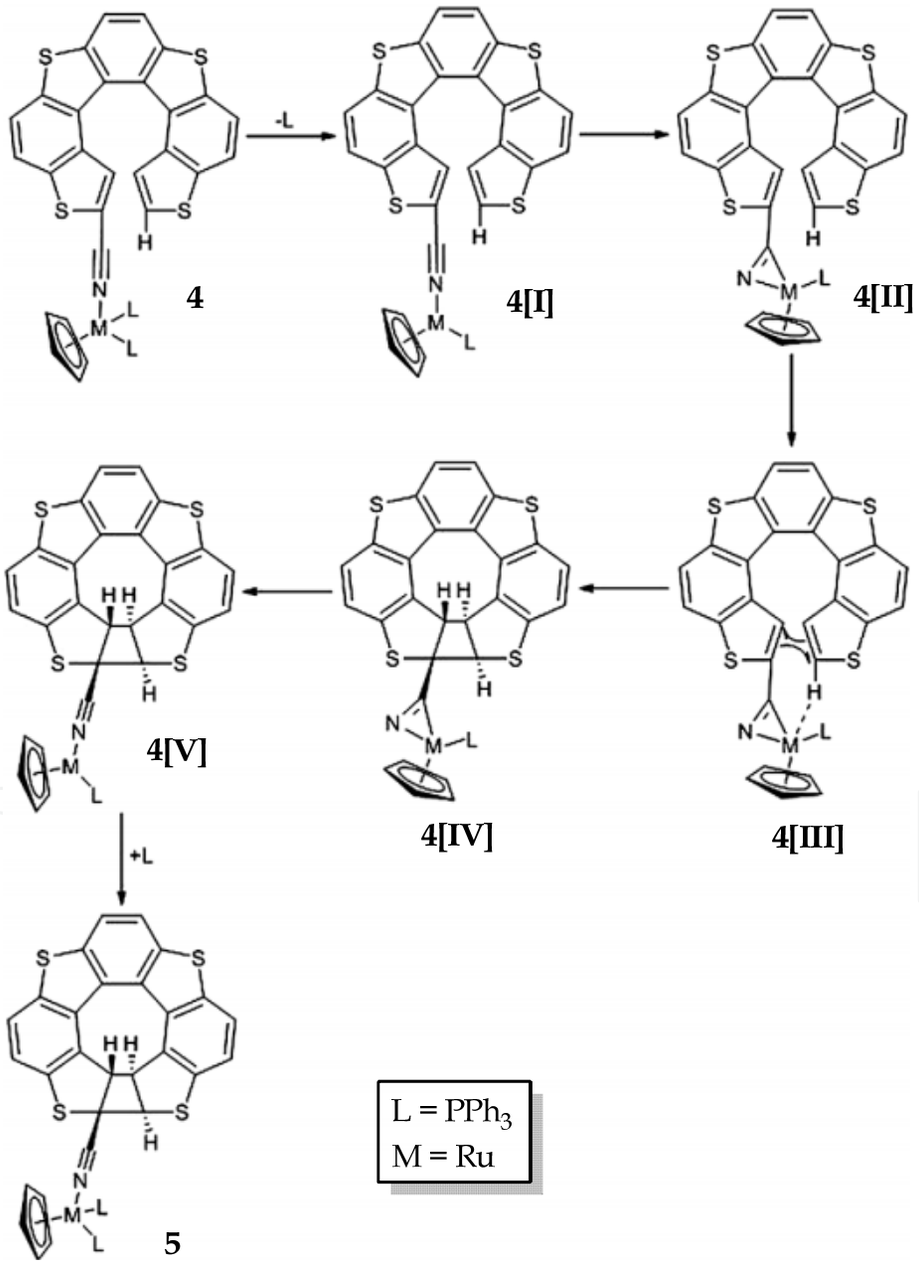

Scheme 2. Reaction mechanism for formation of **5** "Garcia et al., 2009)".

Tetrathia-[7]-helicene **1** have been used for the synthesis of organometallic complexes "(Garcia et al., 2009)". A series of organometallic complexes possessing tetrathia-[7]-helicene nitrile derivative ligands **5** as chromophores, has been synthesized and fully characterized by Garcia et al. "(Garcia et al., 2009)". This compound was analyzed by means of ^{1}H NMR, FT-IR, UV–Vis and X-ray crystallography techniques. The spectroscopic data of this compound was shown with in order to evaluate the existence of electronic delocalization from the metal centre to the coordinated ligand to have some insight on the potentiality of this compound as non-linear optical molecular materials. Slow crystallization of compound **4** revealed an interesting isomerization of the helical ligand with formation of two carbon-carbon bonds between the two terminal thiophenes, leading to the total closure of the helix **5**. The reaction mechanism for the formation of **5** is shown in Scheme 2. Crystal structure of **5** is shown in Figure 3. A selected bond length, angles and torsion angles for compound **5** is summarized in Table 1 "Garcia et al., 2009)".

Another example about helicenes is the hexahelicene **2** and its derivatives that is a chiral molecule "(Noroozi Pesyan, 2006; Smith & March, 2001)". A convenient route for the synthesis of [7]-helicene (**6a**) and [7]-bromohelicene (**6b**) is reported "(Liu et al., 1991)". The crystal structure of 6b is shown in Fig. 4. The crystal structure of **6b** and its unusual oxidation reaction product **7** (as a major product) has been reported "(Fuchter et al., 2012)" (Figure 4 and Scheme 3). Alternatively, compound **6** may be an option for a neutral helicene-derived metallocene complex, since the seven-membered benzenoid rings give rise to a scaffold that completes one full turn of the helix with the two terminal rings being co-facial. It has been theoretically predicted and reported that the **6** has potential to bind some metal cation such as Cr, Mo, W, and Pt in a sandwich model "(Johansson & Patzschke, 2009)". Fuchter and co-workers "(Fuchter et al., 2012)" also reported the crystal structure of **7** that obtained via unusual oxidation rearrangement of **6**. In this structure, The bonds within the pyrenyl unit range between 1.3726(19) and 1.4388(14) Å with the exception of one outlier at 1.3512(18) Å for the C(26)–C(27) bond. The C=C double bonds in rings D and E are 1.3603(15) and 1.3417(16) Å respectively, and the C=O bond is 1.2419(14) Å. The structure of **7** revealed the dominant canonical form to have a pyrenyl group consisting of rings A, B, C and H linked by single bonds to a C–C=C–C=C–C=O unit to form rings D and E (Scheme 3). The pyrenyl unit is flat, the sixteen carbon atoms being coplanar. Ring I has four single bonds and two aromatic bonds, and has a folded conformation with the methylene carbon lying ca. 0.87 Åout of the plane of the other five carbons which are coplanar. Aryl ring G forming the five-membered ring J, links to ring I. The planes of the five coplanar atoms of ring I and the four coplanar atoms of ring J are inclined by ca. 108° to each other. The ring of E is slightly distorted in a boat-like fashion with the carbon shared just with ring D and that shared with rings I and J, out of the plane of the other four atoms which are coplanar to within ca. 0.01 Å.

The formula structure of Katz's helical ferrocene **8** is shown in Figure 5 "(Katz & Pesti, 1982; Sudhakar & Katz, 1986)".

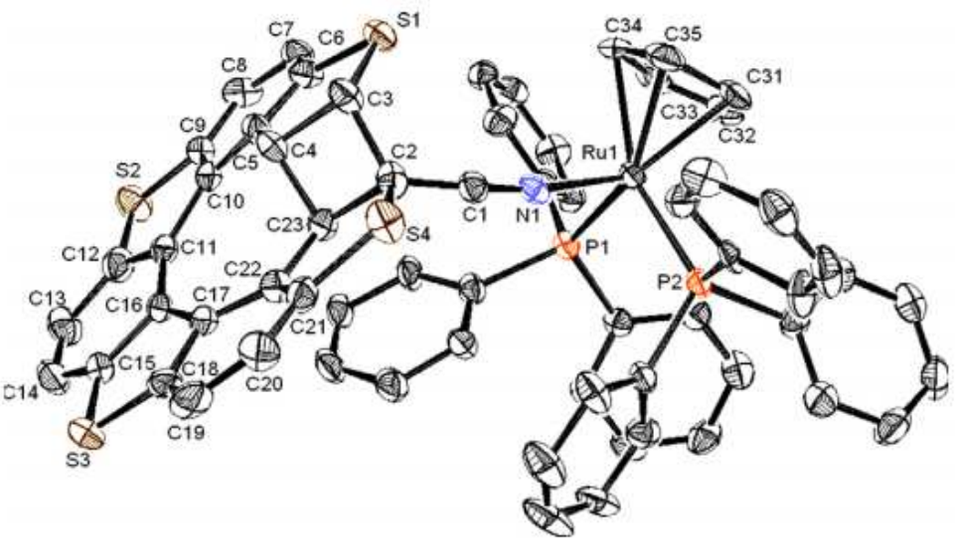

Figure 3. Crystal structure of **5**.

Bond distances (Å)			
Ru(1)–N(1)	2.030(5)	P(2)–C(221)	1.850(7)
Ru(1)–Cp[a]	1.8595(6)	P(2)–C(231)	1.829(6)
Ru(1)–P(1)	2.350(2)	N(1)–C(1)	1.147(8)
Ru(1)–P(2)	2.353(2)	C(1)–C(2)	1.433(9)
P(1)–C(111)	1.843(6)	C(2)–C(3)	1.598(9)
P(1)–C(121)	1.831(7)	C(3)–C(4)	1.535(9)
P(1)–C(131)	1.817(7)	C(4)–C(23)	1.519(9)
P(2)–C(211)	1.846(7)	C(23)–C(2)	1.565(9)
Bond angles (°)			
N(1)–Ru(1)–Cpa	121.79(14)	C(1)–C(2)–C(3)	115.3(6)
N(1)–Ru(1)–P(1)	87.93(14)	C(2)–C(3)–C(4)	88.8(5)
N(1)–Ru(1)–P(2)	90.83(15)	C(2)–C(23)–C(4)	90.6(5)
P(1)–Ru(1)–P(2)	99.84(6)	C(3)–C(4)–C(23)	91.2(5)
P(1)–Ru(1)–Cpa	124.15(5)	C(3)–C(2)–C(23)	87.2(5)
P(2)–Ru(1)–Cpa	122.98(5)	C(5)–C(4)–C(23)	106.9(6)
Ru(1)–N(1)-C(1)	169.9(5)	C(4)–C(23)–C(22)	107.7(5)
N(1)–C(1)–C(2)	175.7(7)	C(2)–C(3)-S(1)	119.3(5)
C(1)–C(2)–C(23)	116.4(6)	C(3)–C(2)–S(4)	116.5(5)
Torsion angles (°)			
Ru(1)–N(1)–C(1)–C(2)	29(11)	N(1)-C(1)–C(2)–C(23)	62(9)
N(1)–C(1)–C(2)–C(3)	-38(9)	C(2)–C(3)–C(4)–C(23)	-11.0(5)
N(1)–C(1)–C(2)–S(4)	-175(9)		

[a] Cp ring centroid.

Table 1. Selected bond distances and bond and torsion angles for compound **5** "(Garcia et al., 2009)".

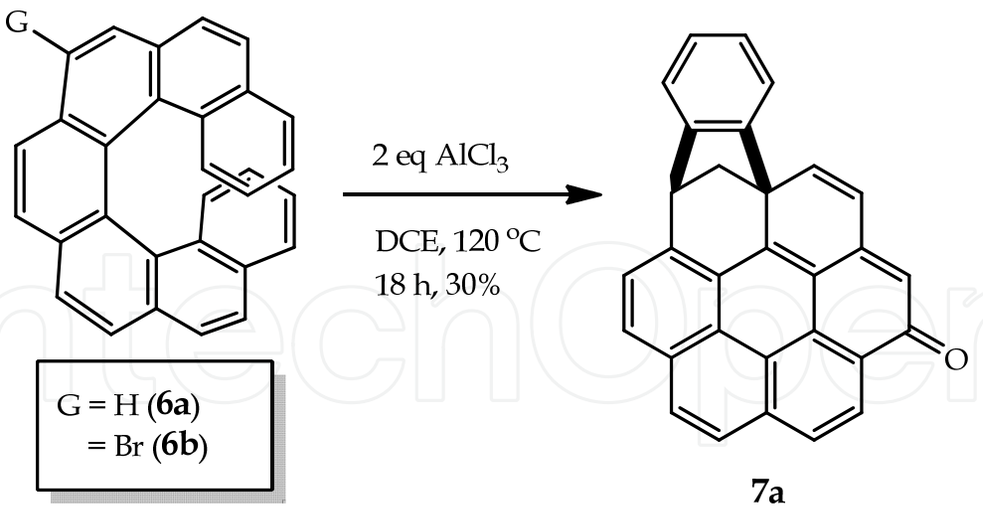

Scheme 3. The formula structures of **6a** and **6b** and its unusual reaction for synthesis of **7a** (and also its structure).

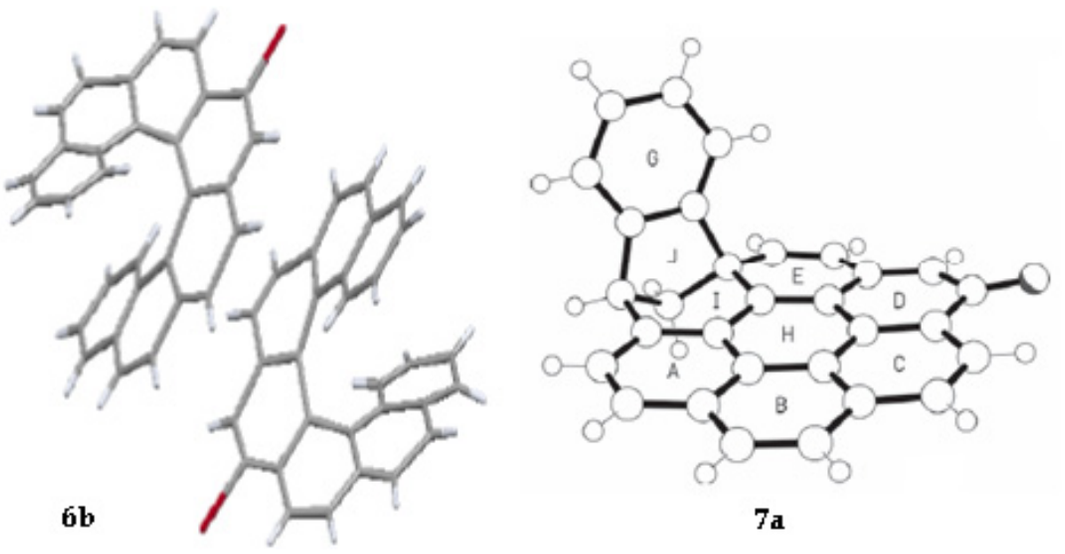

Figure 4. Crystal structures of **6b** and **7a**.

8

Katz's helical ferrocene

Figure 5. The formula structure of Katz's helical ferrocene **8**.

Diazepinone dervatives are of pharmaceutical compounds. Another interesting helical diazepinone compound that is discussed in this section, is 1,9-dimethyl-4,5-dihydro-6*H*-pyrido[3',2':4,5]thieno[2,3-*f*]pyrrolo[1,2-*a*][1,4]diazepin-6-one (**9**). This molecule show two crystallographically independent molecules that form the asymmetric unit of the structure are shown in Figure 6. The X-ray crystallographic analysis shows the molecular structure of the compound **9** and reveals an interesting fact that this structure features two stereochemically different molecules (**9A** and **9B**) that can be understood as different torsion helicoids (Figure 6). The compound has two stereoisomers (*R* and *S* conformers). In each structure the seven-membered diazepinone ring exhibits a boat conformation.

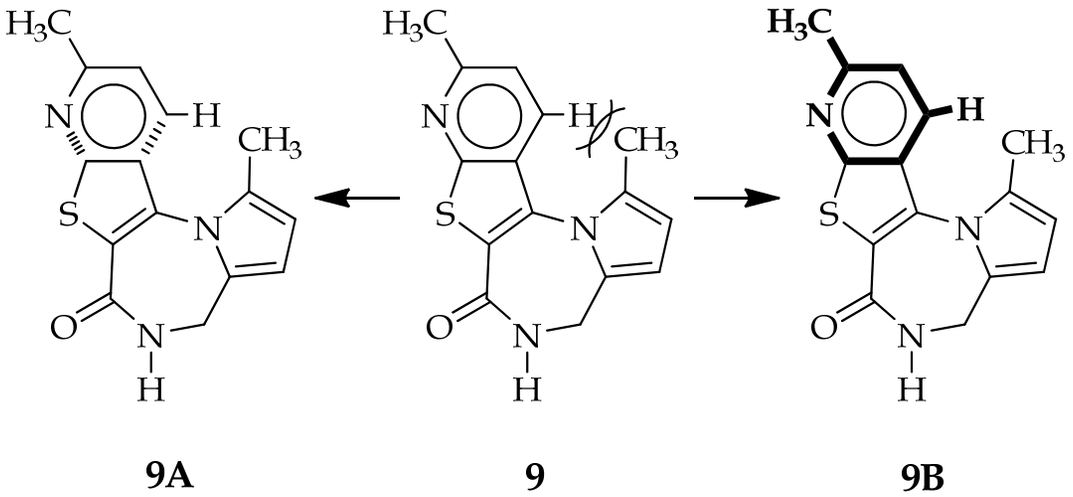

Scheme 4. Two possible different torsion helicoids of **9**.

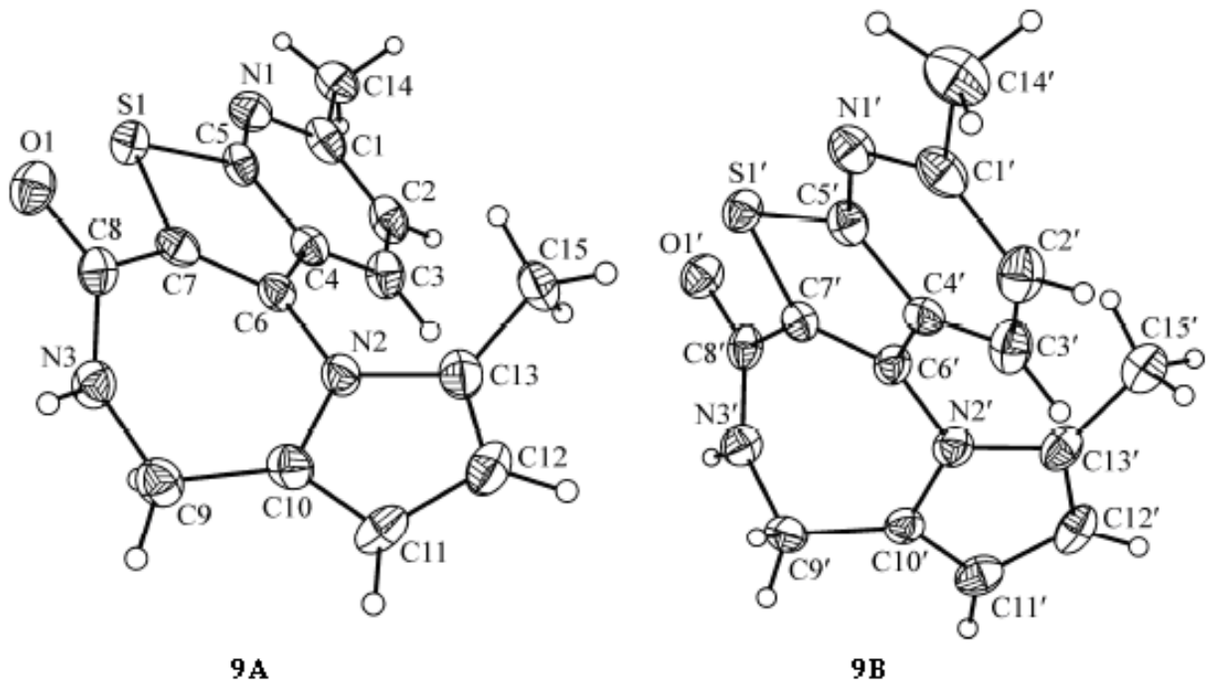

Figure 6. Two independent molecules of **9** in the crystal studied.

The fused pyrido[3',2':4,5]thieno ring moiety has planar geometry. The C3–H3 bond is slightly off the fused pyrido[3',2':4,5]thieno ring plane. The hindrance repulsion between the hydrogen atom at C3 on pyridine ring and methyl group on pyrrole ring makes the molecule of **9** essentially non-planar (repulsion of C3–H3A with C15 and C3'–H3'B with C15' of methyl groups) (Scheme 4). The torsion angles between the pyrrole and thiophene rings in **9A** and **9B** are 45.7(6)° and –49.3(6)°, respectively "(Noroozi Pesyan, 2010)".

The –NH– group of each molecule (e.g. molecule **9A**) makes an intermolecular hydrogen bond to the C=O functional group of the molecule of another kind (molecule **9B**), and *vice versa*. For example, the intermolecular hydrogen bond N3–H3····O1' involves the N3 atom from molecule **9A** and O1' atom from the carbonyl group of molecule **9B**, and *vice versa* for N3'–H3'····O1 (Figure 7). The crystal packing diagram indicates zigzag hydrogen-bonded chains along the crystallographic axes with two distinct hydrogen bonds (Figure 7). The intermolecular hydrogen bonds play a principal and important role in the crystal packing diagram of **9** "(Noroozi Pesyan, 2010)".

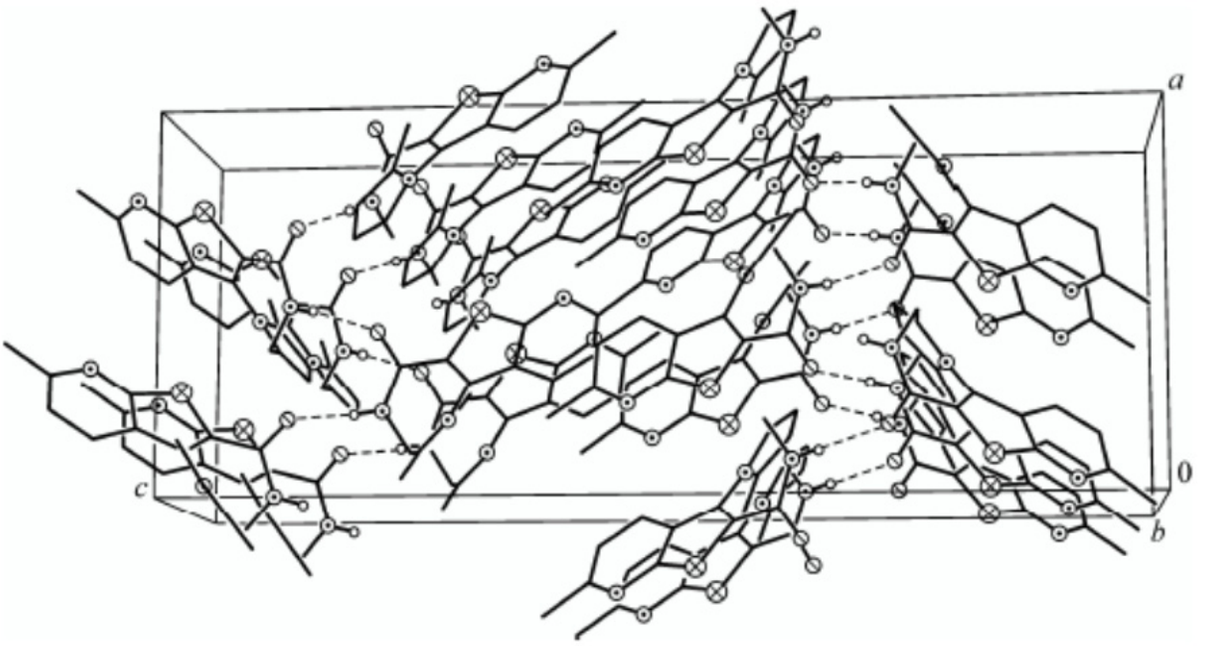

Figure 7. Crystal packing diagram of **9** showing zigzag H-bonds (shown by dashed lines).

One of the most interesting helical primary structure is sown in Figure 8 has been reported by Fitjer et al. "(Fitjer et al., 2003)". Helical primary structures of spiro annelated rings are unknown in nature but have been artificially produced, both in racemic and enantiomerically pure form. The formula structure of 1-cyclobutylidenespiro[3.3]heptane (**10**) as a starting material is shown in Scheme 5. The compound **10** yielded enantiomeric mixture of **11** and **12** in the presence of zinc and 2,2,2-trichloroacetyl chloride. Reductive dehalogenation of **11** and **12** then Wolff–Kishner reduction yielded the desired trispiro[3.0.0.3.2.2]tridecane [rac-(**15**), (symmetry, C_2)]. The crystal structure of the camphanic acid derivative of **15** ((1*S*,5'*S*,10'*S*)-**16**) is shown in Figure 8 "(Fitjer et al., 2003)".

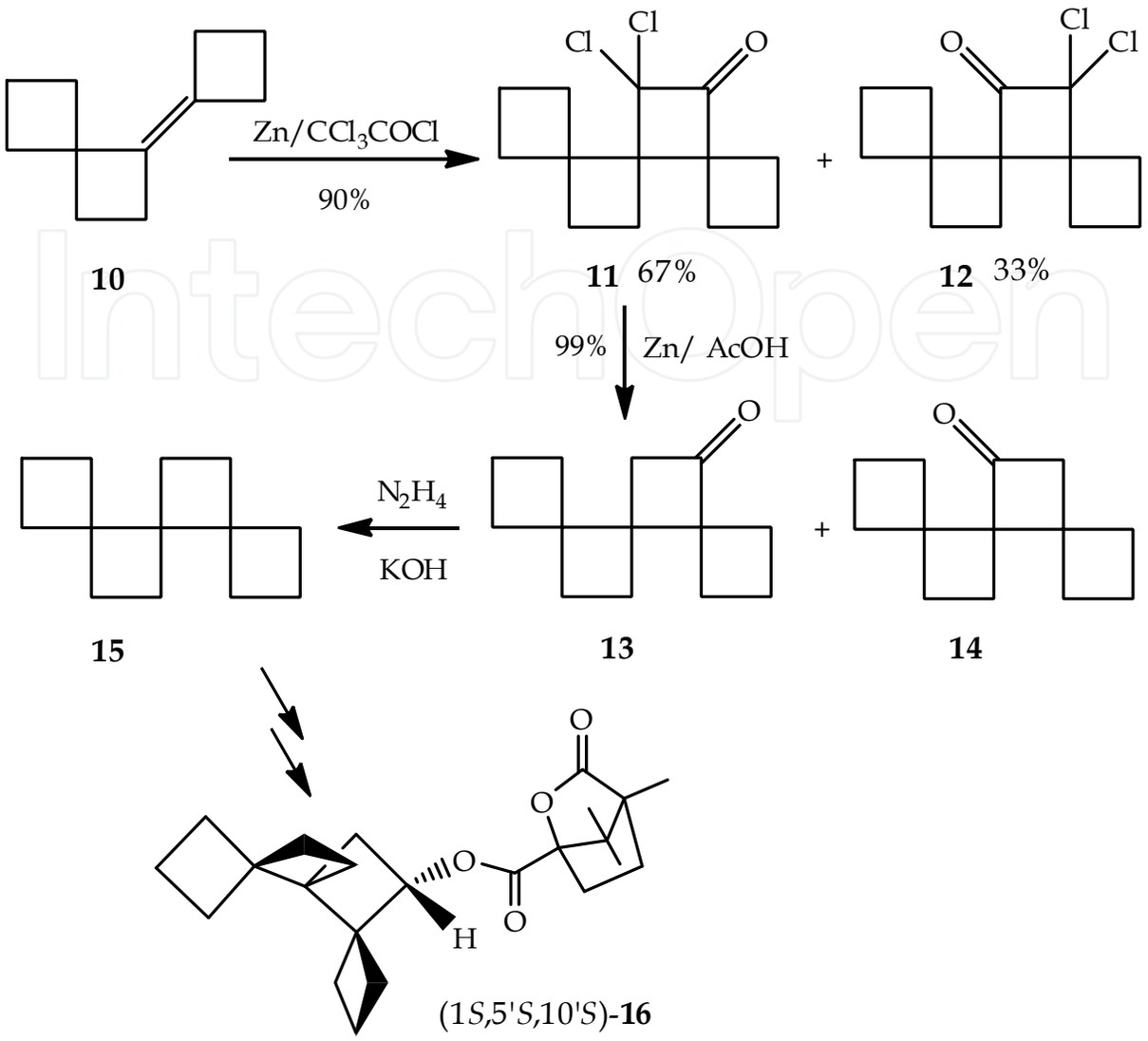

Scheme 5. Synthesis of the compounds trispiro[3.0.0.3.2.2]tridecane (**15**) and the formula structure of its derivative (1*S*,5'*S*,10'*S*)-**16** "(Fitjer et al., 2003)".

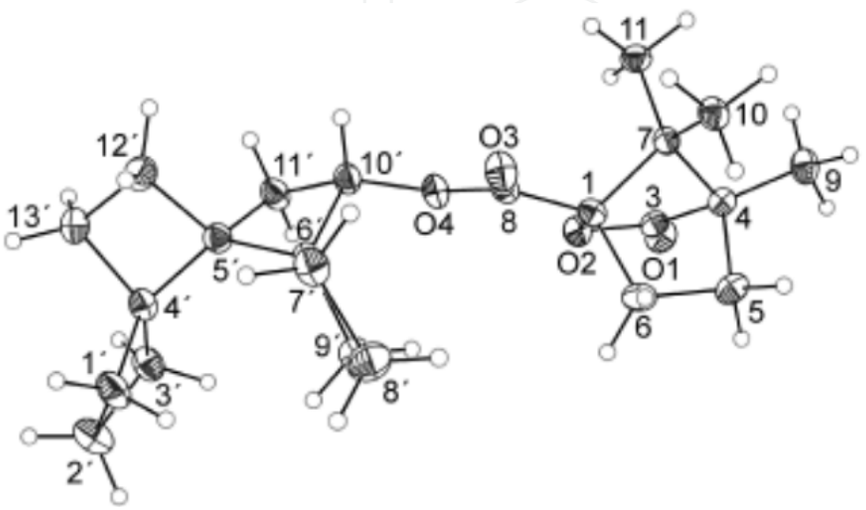

Figure 8. Crystal structure of **(1*S*,5'*S*,10'*S*)-16**.

Helquats, the family of *N*-heteroaromatic cations "(Arai & Hida, 1992)", recently were introduced helical dications that represent a missing structural link between helicenes and viologens"(Casado et al., 2008)". Specifically, basic [7]-helquat (**17**) "(Severa et al., 2010)" is a structural hybrid between [7]-helicene and a well-known herbicide diquat (Scheme 6). Synthesis of [7]-helquat (**17**) starts with bisquaternization of bis-isoquinoline precursor (**18**) with an excess of 3-butynyltriflate followed by the key metal catalyzed [2+2+2] cycloisomerization of the resulting triyne, formed **17** (Scheme 7).

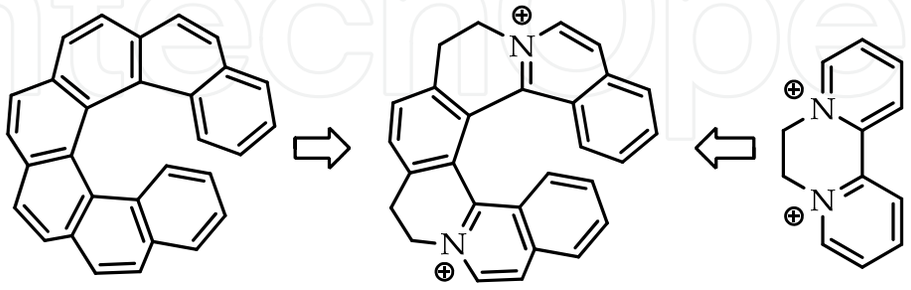

6a [7]helquat **(17)**

Scheme 6. Structural relation of [7]-helquat (**17**) to [7]-helicene **6a** and herbicide diquat.

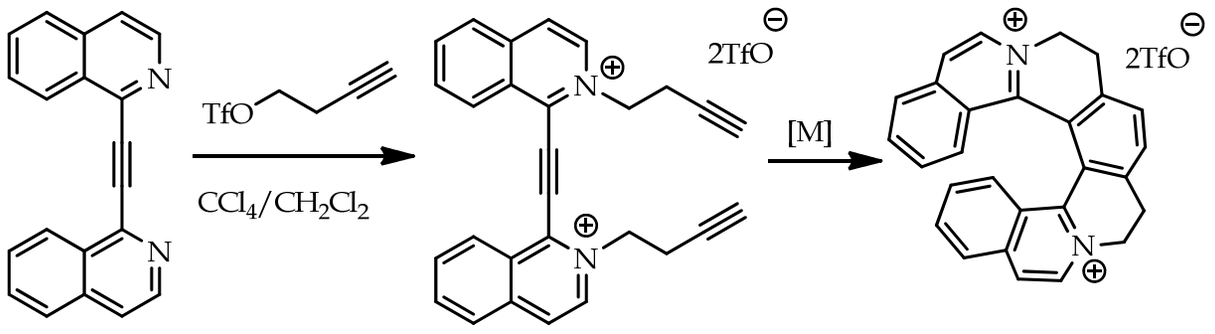

18 **17**

Scheme 7. Synthesis of **17** via one-pot bis-quaternization of **18**.

Recently, Nakano et al. have been reported the helical structure, λ^5-phospha [7]-helicenes 9-phenyl-9*H*-naphtho[1,2-*e*]phenanthro[3,4-*b*]phosphindole-9-oxide (**21**) and its thio analogue 9-phenyl-9*H*-naphtho[1,2-*e*]phenanthro[3,4-*b*]phosphindole-9-sulfide (**22**) "(Nakano et al., 2012)". The formula structure of **21** and **22** and the crystal structure of **21** are shown in Fig. 10. Phospha [7]-helicenes **21** and **22** have more distorted structures than the other heterohelicenes. In the structure of **21**, the sums of the five dihedral angles that are derived from the seven C–C bonds [C(17)-C(17a)-C(17b)-C(17c), C(17a)-C(17b)-C(17c)-C-(17d), C(17b)-C(17c)-C(17d)-C(17e), C(17c)-C(17d)-C(17e)-C(17f), and C(17d)-C(17e)-C(17f)-C(1)] are 95.28 for **21** and 99.68 for **22**. These angles are larger than those of hetero[7]-helicenes **23–25** (79–88°). This case can be attributed to the large angles between the two double bonds of phosphole oxide (50°) and phosphole sulfide (50°) relative to furan (32°), pyrrole (35°), and thiophene (45°). Owing to the larger angle, a larger overlap of the two terminal benzene rings was occurred in the λ^5-phospha[7]-helicenes, therefore, a stronger steric repulsion. These larger distortions in **21** and **22** explain the higher tolerance of **21** and **22** towards racemization.

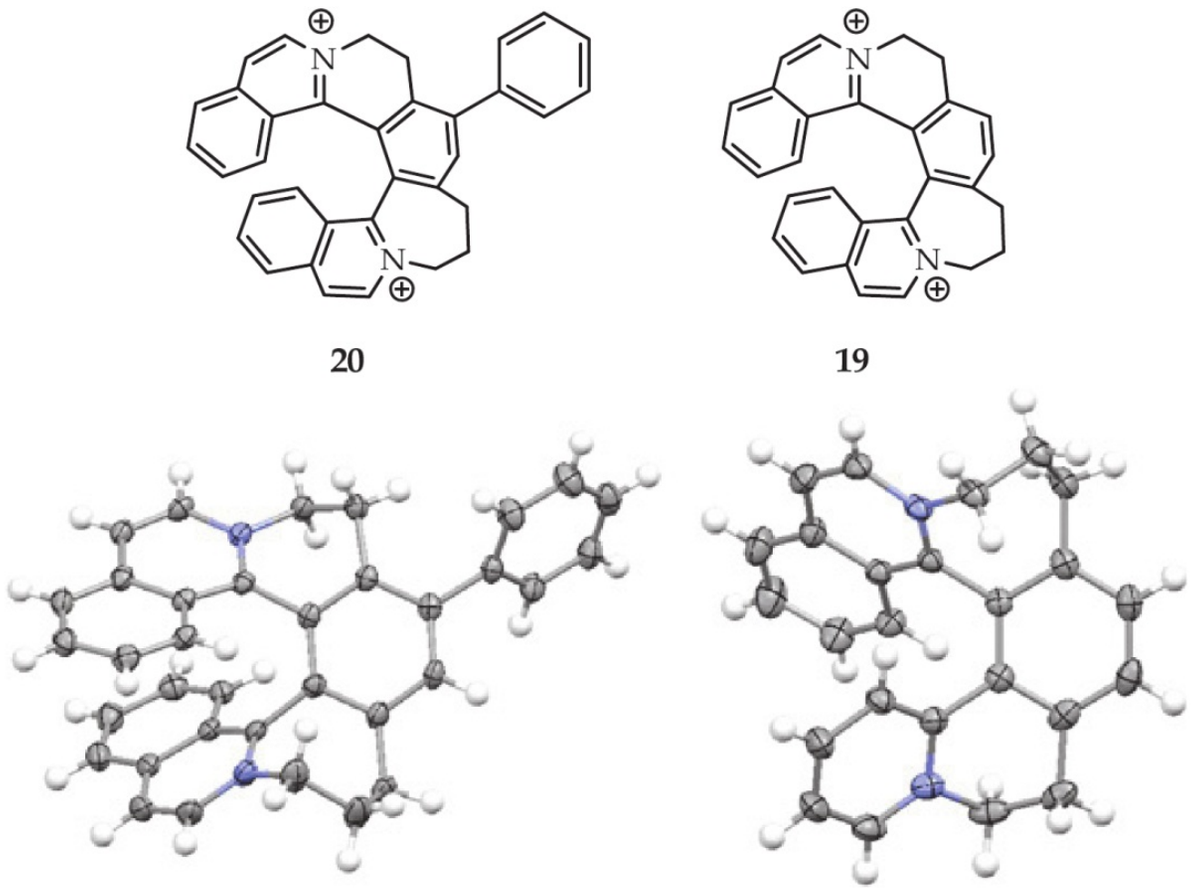

Figure 9. Formula and X-ray single crystal structure of compounds **19** and **20** (Triflate counterions are omitted for clarity) "(Severa et al., 2010)".

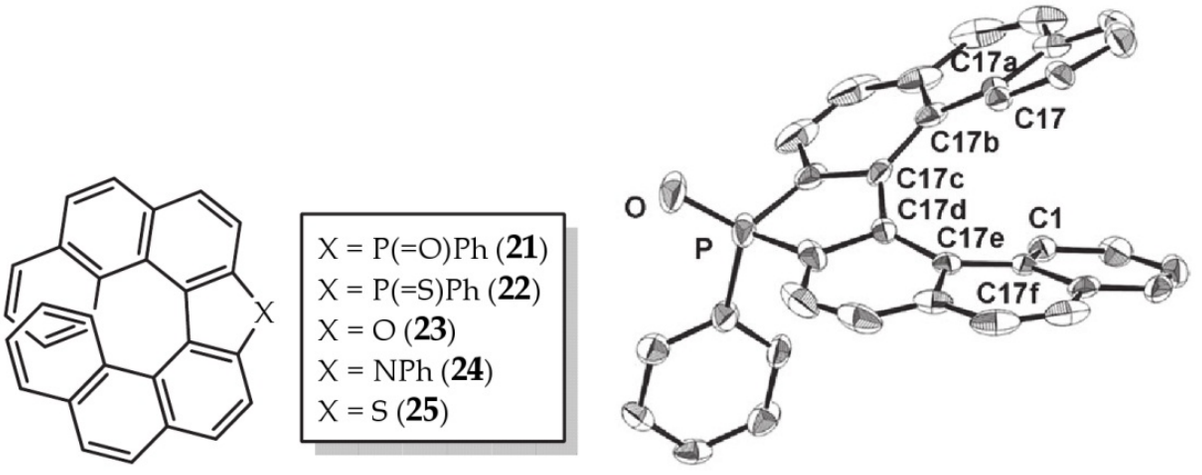

Figure 10. Formula structures of λ^5-Phospha[7]-helicenes **21** and **22** and crystal structure of **21** as representative.

2.2. Inter- and intramolecular hydrogen bonds in the crystal structure of organic compounds

Hydrogen bond plays a key and major role in the biological and pharmaceutical systems and remains a topic of intense current interest. Few selected recent articles exemplify the general scope of the topic, ranging from the role of H-bonding such as in: weak interaction in gas phase "(Nishio, 2005; Wang et al., 2005)", supramolecular assemblies "(McKinlay et al., 2005)", helical structures "(Azumaya et al., 2004; Noroozi Pesyan, 2010)". Important consequences of both inter- and intra-molecular H-bonding have long been recognized in the physicochemical behavior of DNA and RNA "(Jeffery & Saenger, 1991)".

Several kinds of hydrogen bond have been reported. If the donor-acceptor distance to be in the range of; 2.50 ≤ d (O···O) ≤ 2.65, this kind of hydrogen bond is strong and when shorter than 2.50 Å (d(O···O)≤ 2.50), to be very strong hydrogen bond "(Gilli et al., 1994)".

In very short O···H···O bonds (2.40-2.45 Å) the major distribution of the proton are as follows:

i. The proton is closer to one of the O atoms (asymmetric hydrogen bond).
ii. The proton is located precisely at the centre (symmetric or centred hydrogen bond).
iii. There is statistically disorder of the proton between two positions on either side of the centre (the proton is closer to one or the other side in different domains of the crystal).
iv. There is a dynamical disorder between two positions as in (iii); the proton jumps between the two positions in the same hydrogen bond "(Gilli et al., 1994; P. Gilli & G. Gilli, 2000; Olovsson et al., 2001; Steiner, 2002)".

For instance, the structure of the potassium hydrogen dichloromaleate (**26**) has been studied by neutron diffraction at 30 and 295 K, with the emphasis on the location of the protons. There are two crystallographically independent hydrogen atoms in two very short hydrogen bonds, 2.437(2) and 2.442(2) Å at 30 K. For the centrosymmetric space group P1, with the hydrogen atoms located at the centres of symmetry, the structure could be refined successfully. Olovsson et al. have then been applied several different types of refinements on this structure, including unconventional models; with all atoms except hydrogen constrained in P1, but with hydrogen allowed to refine without any constraints in P1, anisotropic refinement of all atoms resulted in clearly off-centred hydrogen positions. The shifts of the two hydrogen atoms from the centres of symmetry are 0.15(1) and 0.12(1) Å, respectively, at 30 K, and 0.15(1) Å for both hydrogen atoms at room temperature. At 30 K: R(F) = 0.036 for 1485 reflections; at 295 K: R(F) = 0.035 for 1349 reflections (Olovsson et al., 2001)" (Fig. 11).

One of the most interesting example about intermolecular hydrogen bond is the heptan-4-yl (2'-hydroxy-[1,1'-binaphthalen]-2-yl) phosphonate (**27a**) "(Dabbagh et al., 2007)". The phosphonate **27a** was existed in dimmer form via two strong intermolecular hydrogen bonds with centrocymmetric (C_i) 18-membered dimmer form consisting of two monomers strongly hydrogen-bonded between the oxygen of P=O units and hydroxyl hydrogen atoms (Fig. 12). The crystal structure of **27a** was determined by X-ray crystallography and is shown

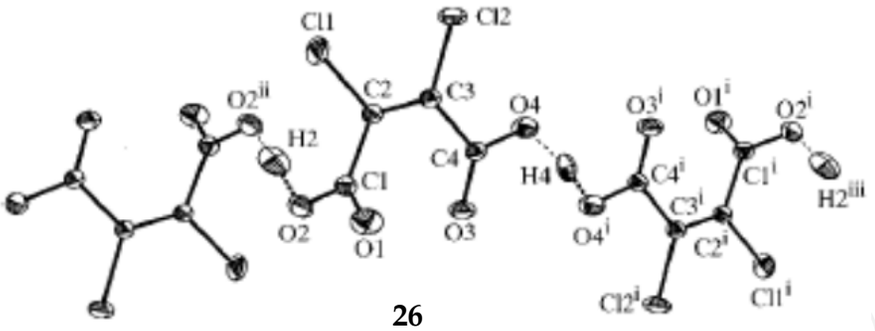

26

Figure 11. Crystal structure of potassium hydrogen dichloromaleate (**26**).

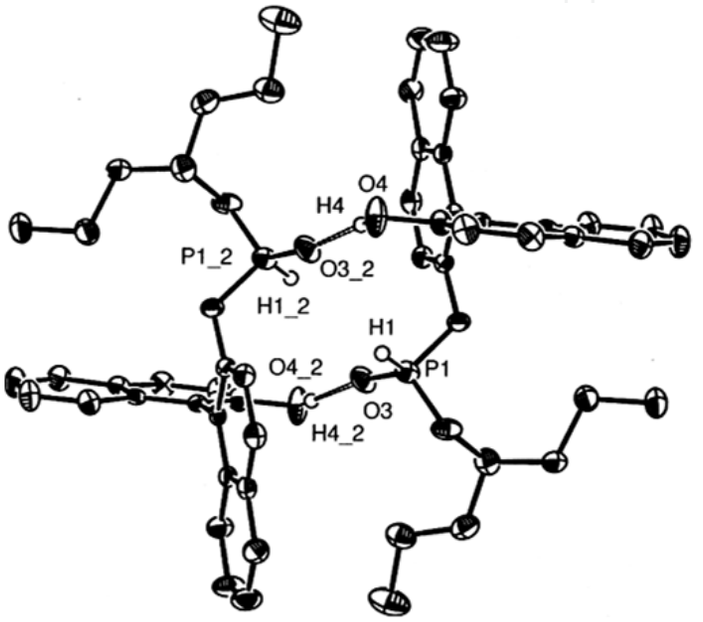

Figure 12. Crystal structure of **27a**.

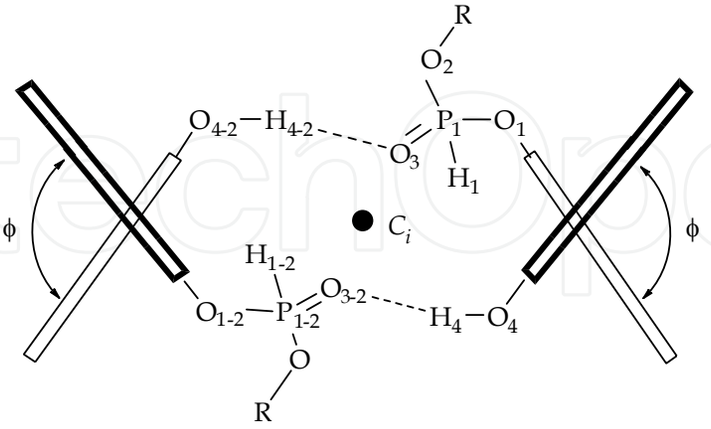

27

R: 4-Heptyl (**a**), cyclohexyl (**b**)

Figure 13. Representatively, two strong intermolecular hydrogen bonds with centrocymmetric 18-membered dimmer form in **27a** and **27b**.

in Fig. 12. The selected bond lengthes, angles and torsion angles of **27a** are summarized in Tables 2-4, respectively. Crystal data indicated the torsion angles (ϕ) between two naphthalenic rings moieties in BINOL species are 95.28(16)° and are transoid forms (Fig. 13). The intermolecular hydrogen bond distance in the structure of **27a** was obtained 2.70 Å (strong hydrogen bond) and comparised with other hydrogen bonds P-containing systems (Table 5).

Entry	Bond	length (Å)
1	P(1) – O(3)	1.4578(11)
2	P(1) – O(2)	1.5544(12)
3	P(1) – O(1)	1.5865(11)
4	P(1) – H(1)	1.295(16)
5	O(1) – C(1)	1.4073(17)
6	O(2) – C(21)	1.5006(19)
7	O(4) – C(12)	1.3634(18)
8	O(4) – H(4)	0.89(2)
9	O(3) – H(4)	1.81(2)
10	C(10) – C(11)	1.4942(19)

Table 2. Selected bond length (Å) of dimmer **27a**.

Entry	Bond	Angle (θ, °)
1	O(3) – P(1) – O(2)	118.32(7)
2	O(3) – P(1) – O(1)	113.50(7)
3	O(2) – P(1) – O(1)	102.16(6)
4	O(3) – P(1) – H(1)	112.7(7)
5	O(2) – P(1) – H(1)	103.9(7)
6	O(1) – P(1) – H(1)	104.7(8)
7	C(1) – O(1) – P(1)	122.24(9)
8	C(21) – O(2) – P(1)	122.27(10)
9	C(12) – O(4) – H(4)	114.4(14)
10	C(10) – C(1) – C(2)	123.47(14)
11	C(10) – C(1) – O(1)	117.78(13)
12	C(2) – C(1) – O(1)	118.66(13)
13	C(9) – C(10) – C(11)	120.98(12)
14	O(4) – C(12) – C(11)	124.08(14)
15	O(4) – C(12) – C(13)	114.68(13)
16	O(2) – C(21) – C(22)	107.92(12)
17	O(2) – C(21) – C(25)	111.86(18)
18	C(22) – C(21) – C(25)	108.84(18)
19	O(2) – C(21) – H(21)	109.4
20	C(22) – C(21) – H(21)	109.4
21	C(25) – C(21) – H(21)	109.4

Table 3. Selected bond angle of dimmer **27a**.

Entry	Bond	Torsion angles (*Φ*, °)
1	O(3) – P(1) – O(1) – C(1)	51.11(13)
2	O(2) – P(1) – O(1) – C(1)	179.64(11)
3	O(3) – P(1) – O(2) – C(21)	58.93(13)
4	O(1) – P(1) – O(2) – C(21)	-66.49(12)
5	P(1) – O(1) – C(1) – C(10)	110.03(13)
6	P(1) – O(1) – C(1) – C(2)	-73.13(15)
7	O(1) – C(1) – C(2) – C(3)	-177.12(12)
8	C(7) – C(8) – C(9) – C(10)	178.21(14)
9	C(2) – C(1) – C(10) – C(11)	-178.59(12)
10	O(1) – C(1) – C(10) – C(11)	-2.11(19)
11	C(1) – C(10) – C(11) – C(12)	-97.30(17)
12	C(9) – C(10) – C(11) – C(12)	83.69(18)
13	C(1) – C(10) – C(11) – C(20)	83.73(17)
14	C(9) – C(10) – C(11) – C(20)	-95.28(16)
15	C(20) – C(11) – C(12) – O(4)	179.63(140
16	C(10) – C(11) – C(12) – O(4)	0.6(2)
17	P(1) – O(2) – C(21) – C(22)	-119.33(13)
18	P(1) – O(2) – C(21) – C(25)	120.97(19)
19	O(2) – C(21) – C(22) – C(23)	62.75(18)
20	C(25) – C(21) – C(22) – C(23)	-175.66(19)
21	C(21) – C(22) – C(23) – C(24)	166.78(15)
22	O(2) – C(21) – C(25) – C(26)	-68.8(3)
23	C(22) – C(21) – C(25) – C(26)	172.0(2)
24	C(21) – C(25) – C(26) – C(27)	-173.4(3)

Table 4. Selected torsion angles of dimmer **27a**.

Linkages	Bond distance [Range, donor….H….acceptor] (Å)	Strength
P–O–H....O–P	2.39-2.50	Very strong
P–O–H....O–P	2.50-2.65	Strong
P–O–H....O–C	2.41-2.82	Strong
P–H....OH_2	2.56-3.15	Moderate
P–O....H–N	2.65-3.10	Moderate
Dimmer **27**	2.70	Strong

Data taken from references "(Corbridge, 1990; Gilli et al., 1994; Gilli & & Gilli, 2000; Steiner, 2002)".

Table 5. Classification of hydrogen bonds within P-containing systems.

Dimeric centrosymmetric ring structures are quite common within phosphorous chemistry: for example; the structures of **28** and **29** are of 12- and 8-membered structures, respectively "(Corbridge, 1990)". According to spectroscopic evidence, esters of (trichloroacetyl) amidophosphoric acid (**29**) exist as **29I** rather than **29II**, which suggests that the hydrogen bond in N-H···O=P is stable than that of in N-H···O=C "(Corbridge, 1990)".

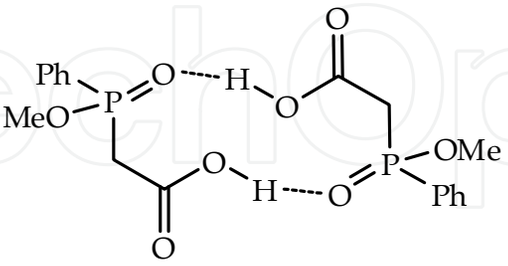

28

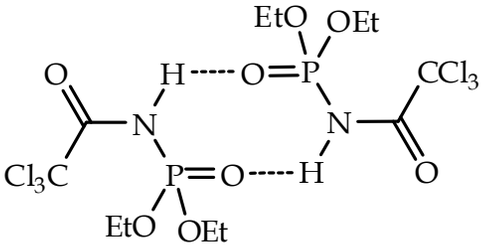

29I

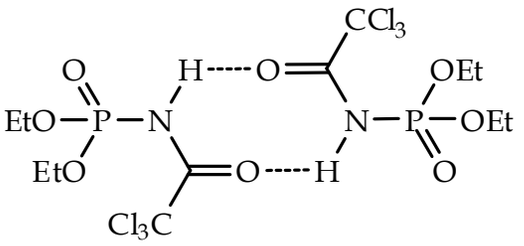

29II

The formula structures of (*E*)-2-benzamido-3-(pyridin-2-yl)acrylic acid (**30a**) and (*E*)-2-benzamido-3-(pyridin-4-yl)acrylic acid (**30b**) are shown in Figure 14. The isomer **30a** possesses a strong seven-membered ring intramolecular hydrogen bonding and shows quite different physicochemical properties, such as solubility and pKa, comparing with its isomer **30b**. The p-conjugation between pyridyl and acrylate moieties is extended by intramolecular hydrogen bonding leading to a strong absorption at about 340 nm. Intramolecular proton transfer facilitates in the excited state, resulting in dual emission at around 420 nm and 490 nm in acetonitrile "(Guo et al., 2011)". Crystal structure of **30a** show a strong seven-membered ring intramolecular hydrogen bonding (Figure 15). The intramolecular proton transfer is facilitated by intramolecular hydrogen bond of O–H···N. Tautomeric forms of **30a** is shown in Scheme 8.

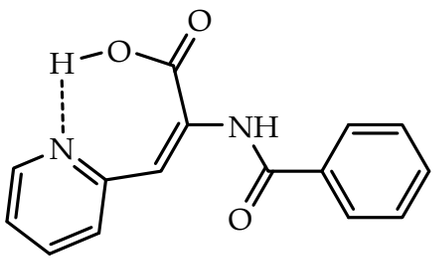

30a

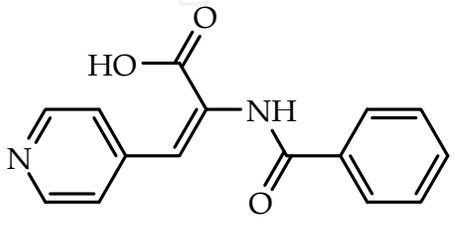

30b

Figure 14. Formula structures of **30a** and **30b**.

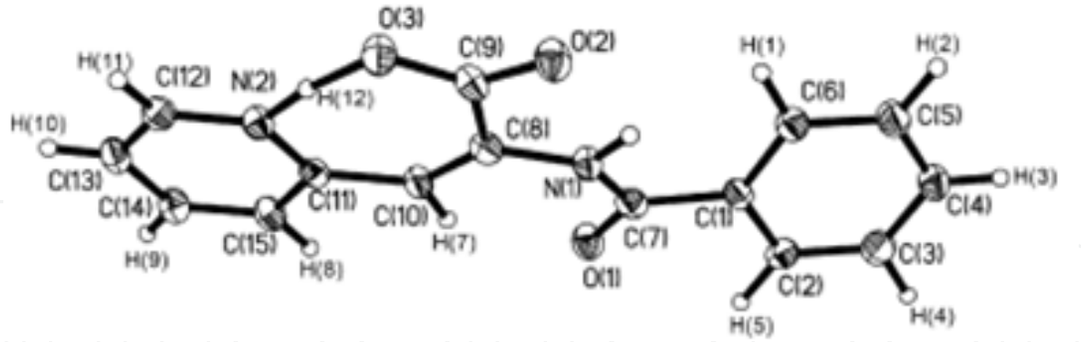

Figure 15. Crystal structure of **30a**.

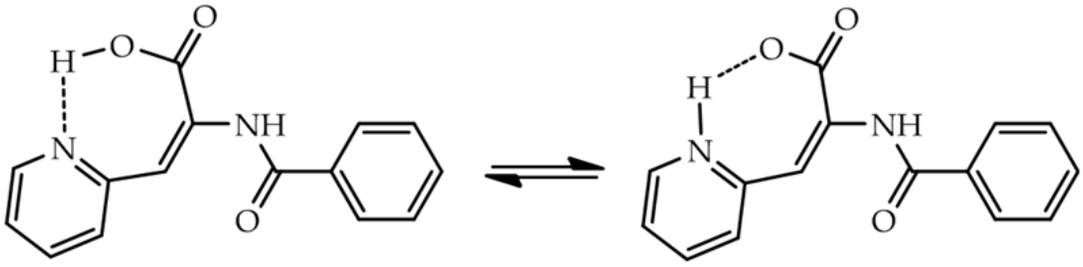

30a[I] **30a[II]**

Scheme 8. Possible tautomeric forms of **30a**.

There is hydrogen bonding between the acrylate O(3) and the pyridine N(2) atoms; the distance between these two atoms is 2.483 Å, and the O(3)-H(12)-N(2) angle is 171.3°. The O(3)-H(12) distance is 1.345 Å (the theoretical distance is 0.920 Å for general carboxyl O-H bond), which is longer than the N(2)-H(12) distance of 1.145 Å (the general distance is 0.960 Å). The distance difference revealed that H(12) is closer to the pyridine N(2) than it is to the acrylate O(3). The O(2)-C(9) and O(3)-C(9) distances are 1.233 Å and 1.272 Å, respectively. These results show that H(12) is involved in a strong intramolecular hydrogen bonding. N(2)-H(12)···O(3), in which the H(12) interaction with the pyridine N(2) is stronger than that with O(3) atom. The carboxylic acid proton moves to the pyridine N atom, while an electron delocalizes across O(2), O(3), and C(9) to form two almost equivalent carbonyl groups. These results provide further evidence that compound **30a** exists mainly as a tautomeric form **30a** (NH) in the solid state (**30a[II]**) form "(Guo, et al. (2011)".

Resorcarene derivatives are used as units in self-assembled capsules via hydrogen bonds. Like to calixarenes, resorcarenes are the core to which specific functional groups are attached. These groups are responsible for the hydrogen bonds while the resorcarenes offer the right spatial arrangement of them. McGillivray and Atwood found that **31** forms in the crystalline state a hexameric capsule with the internal volume of about 1375Å^3. There are 60 hydrogen bonds in hexameric with the help of eight molecules of water (Fig. 16) "(McGillivray & Atwood, 1997)".

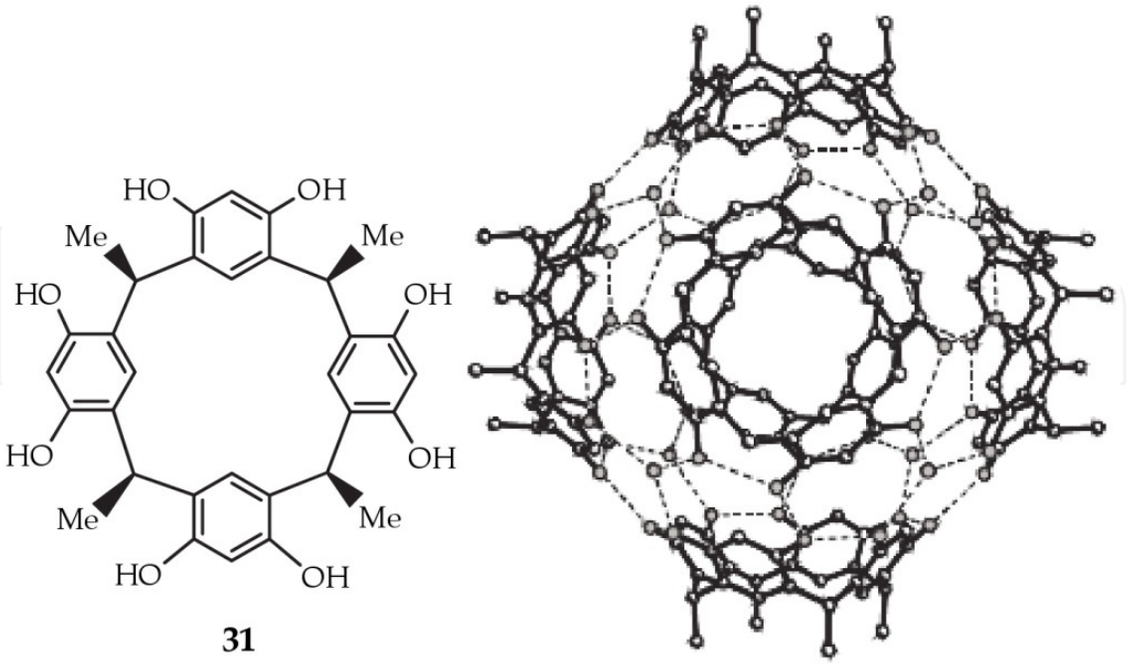

Figure 16. Formula structure of **31** unit and crystal structure of **(31)$_6$·8H$_2$O**.

Yoshida et al. have also been reported the formation of a three-dimensional hydrogen bonding network by self-assembly of the Cu(II) complex of a semi-bidentate Schiff base "(Yoshida et al., 1997)". The crystal structure of the Cu(II) complex of Shiff base **32** is shown in Fig. 17. The infinite overall structure of **32** is found to be organized by a three-dimensional hydrogen-bonding network in which the –NH$_2$·····O$_2$S– type intermolecular hydrogen bonds play an important role, as shown in Fig. 18. One complex molecule is surrounded by four adjacent complexed molecules through four –NH$_2$·····O$_2$S– hydrogen bonds. These hydrogen bonds would be strong judging from the NH····O distances in the range 2.032–2.941 Å. From the neutron diffraction study of sulfamic acid ($NH_3^+SO_3^-$), a comparably strong hydrogen bond has been observed (–N$^+$H·····O–S– distances in the range 1.95–2.56 Å) "(Jeffrey & Saenger, 1991)". Similar hydrogen bonds between sulfone and hydroxyl groups [2.898(6) Å] have been found in a supramolecular carpet formed *via* self-assembly of bis(4,4′-dihydroxyphenyl) sulfone "(Davies et al., 1997)". Furthermore, four weak Br····H hydrogen bonds may participate in the hydrogen-bonding arrays "(Yoshida et al., 1997)".

Yang et al. reported the crystal structure of Bis(barbiturato)triwater complex of copper(II). The neutral Cu(H$_2$O)$_3$(barb)$_2$ molecules are held together to form an extensive three-dimensional network *via* –OH·····O– and –NH·····O– hydrogen-bonded contacts "(Yang et al., 2003)". Hydrogen bonding motifs in fullerene chemistry have been reported by Martín et al. as a minireviewe. The combination of fullerenes and hydrogen bonding motifs is a new interdisciplinary field in which weak intermolecular forces allow modulation of one-, two-, and three-dimensional fullerene-based architectures and control of their function "(Martín et al., 2005)".

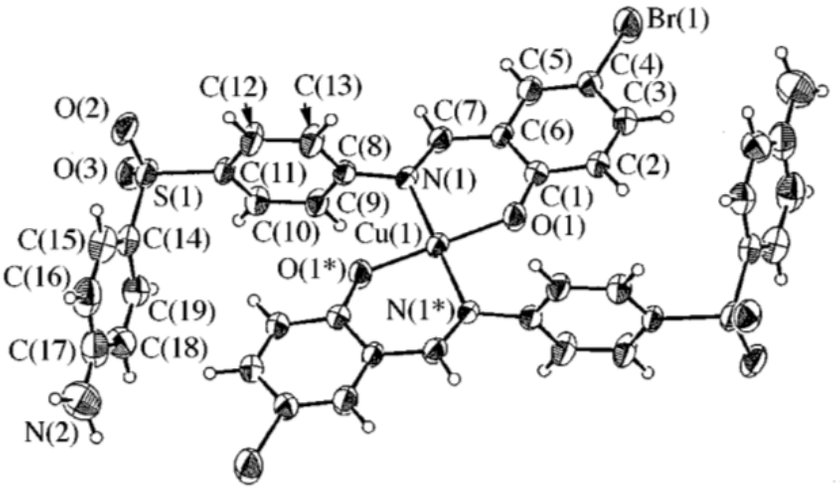

Figure 17. Crystal structure of **32** unit.

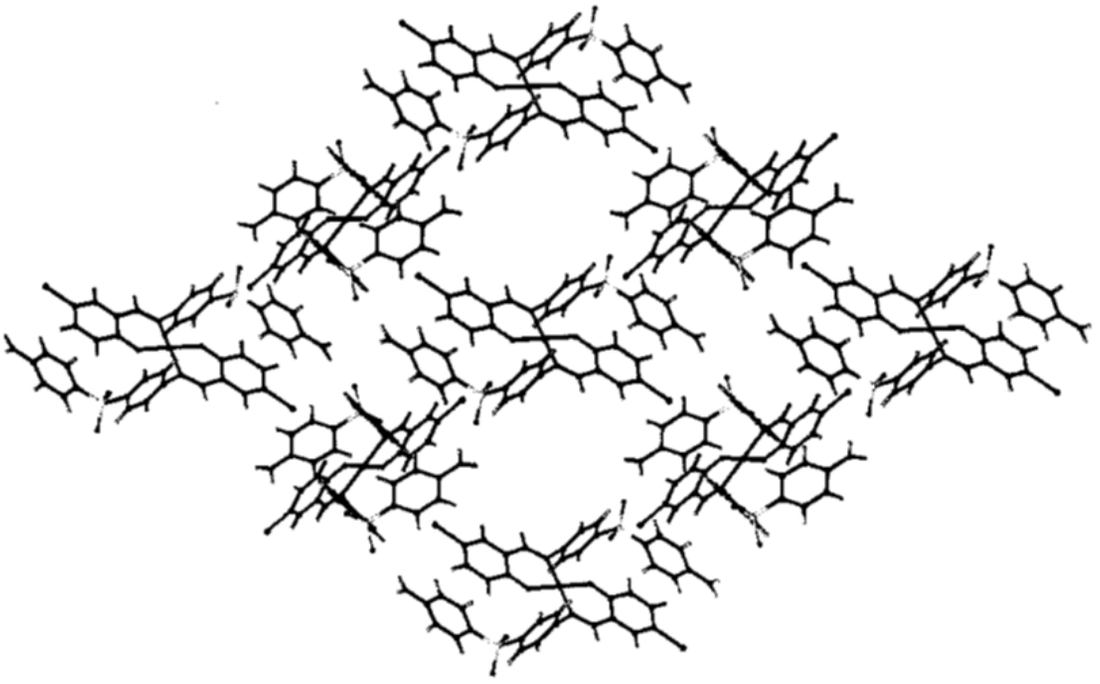

Figure 18. Crystal packing diagram of **32**.

Methyl 2,4-dimethoxy salicylate (**33**) as potential antitumor activity, was synthesized from the reaction of 1,3,5-trimethoxybenzene (the most electron-rich aromatic ring) with 2-methoxycarbonyl-5-(4-nitrophenoxy) tetrazole, under solvent-free conditions, a low yield product was obtained (< 2%), while in the presence of a Lewis acid ($AlCl_3$), the yield was increased to 30% (a kind of trans esterification reaction) "(Dabbagh et al., 2003)".

Crystal structure of **33** is shown in Fig. 19. The carbon-oxygen framework of the molecular structure of **33** is essentially planar; bond lengths and angles are summarized in Table 6, while a structural diagram is shown also in Fig. 20. Planarity is maintained by a strong intramolecular hydrogen bonding interaction between the carbonyl-oxygen and phenolic-H

atom [H(1)····O(1) = 1.68(4) Å; O(5) – H(1) = 1.00(4) Å], and a much weaker intramolecular hydrogen bond of distance 2.535 Å between Me hydrogen's [H(8)] and the C=O group (in what we label a "bisected" conformation with C*s* symmetry, Figs. 19 and 20). The orientations of the *o*-OMe and ester-OMe are such to minimize steric interactions. The structure of **33** was also calculated by semi-empirical *ab-initio*, *PM*3 and *AM*1 methods, and data for bond lengths, angles and torsion angles are in good agreement together with the experimental ones (Tables 6 and 7), while the corresponding calculated H(1)····O(1) bond lengths were 1.57, 1.78 and 1.97 Å,

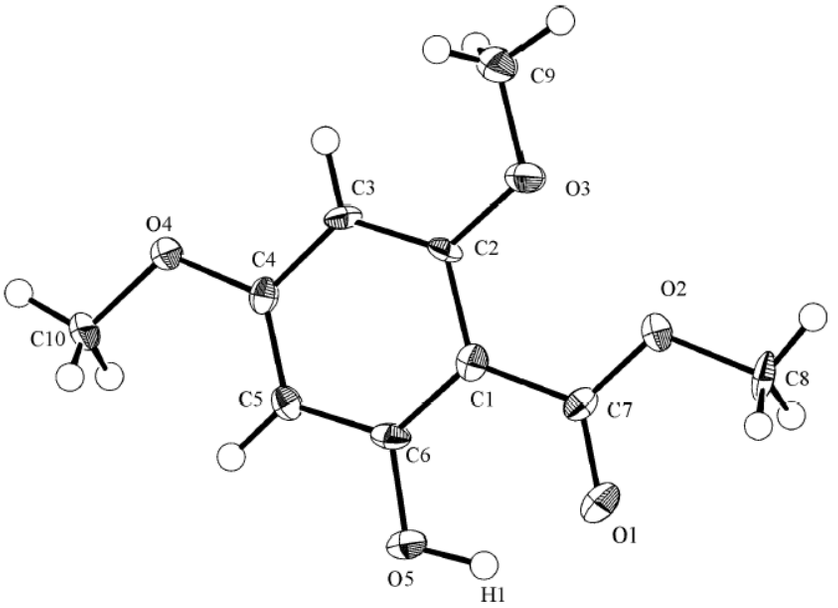

Figure 19. Crystal structure of **33** with 50% probability ellipsoids.

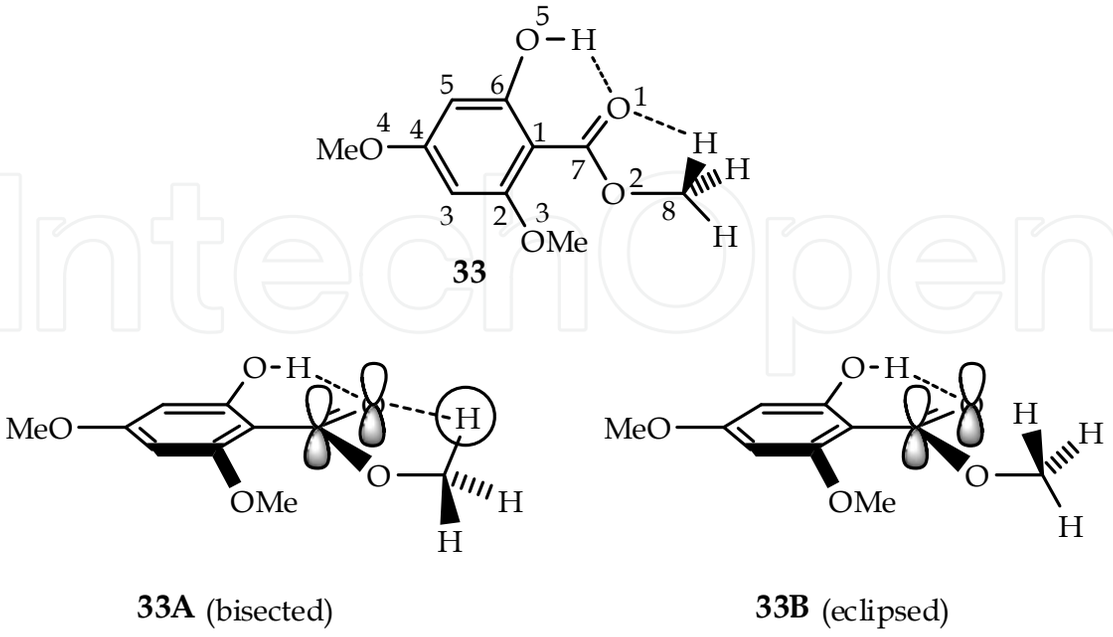

Figure 20. Diagrams showing the favored so-called "bisected" (left) and "eclipsed" (right) conformations of **33**.

and the calculated O(5) – H(1) values were 1.00, 0.980, 0.970 Å, respectively. The *ab-initio* value for the weaker hydrogen bonding interaction was 2.574 Å. The *ab-initio* calculation also revealed a 1.40 Kcal higher energy, eclipsed conformation with C*1* symmetry (Fig. 21 c and d, Fig. 20, Table 7) with an H(8) – carbonyl bond length of 2.14 Å "(Dabbagh et al., 2004)".

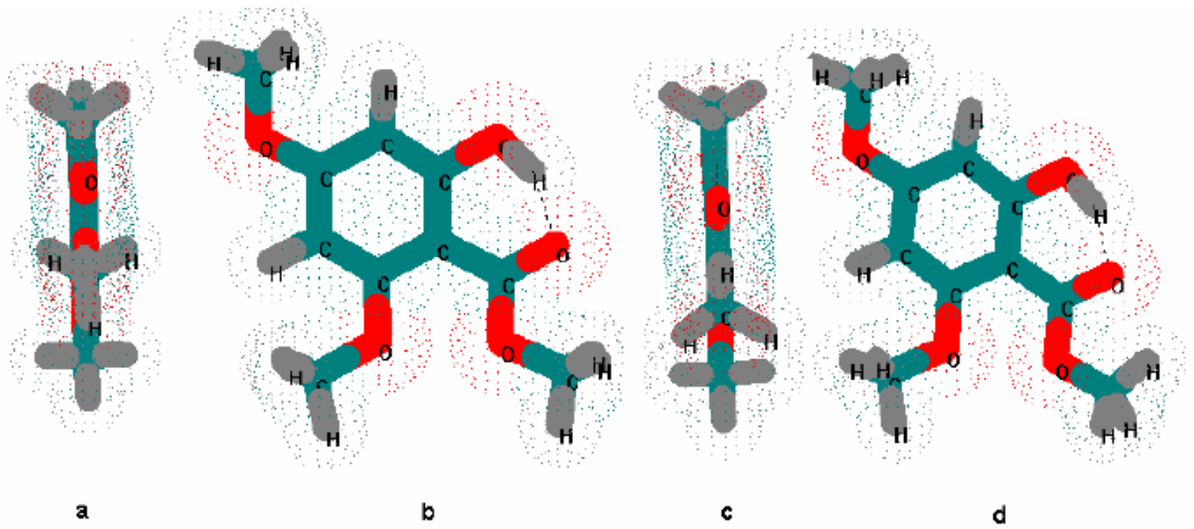

Figure 21. Molecular structures for **33** from *ab-initio* analysis [side-view: **a** (bisected); **c** (eclipsed), and front-view: **b** (bisected0; **d** (eclipsed)].

Atoms	Bond lengths (Å)	Atoms	Bond angles(º)
O(1) – C(7)	1.247(4)	C(7) – O(2) – C(8)	116.1(3)
O(2) – C(7)	1.325(4)	C(2) – O(3) – C(9)	117.1(3)
O(2) – C(8)	1.465(4)	C(4) – O(4) – C(10)	115.8(2)
O(3) – C(2)	1.363(4)	C(2) – C(1) – C(6)	116.9(3)
O(3) – C(9)	1.438(4)	C(2) – C(1) – C(7)	124.7(3)
O(4) – C(4)	1.362(4)	C(6) – C(1) – C(7)	118.3(3)
O(4) – C(10)	1.443(4)	O(3) – C(2) – C(1)	117.1(3)
C(1) – C(2)	1.432(4)	O(3) – C(2) – C(3)	121.9(3)
C(1) – C(6)	1.393(4)	C(1) – C(2) – C(3)	121.03
C(1) – C(7)	1.465(4)	C(2) – C(3) – C(4)	119.8(3)
C(2) – C(3)	1.378(4)	O(4) – C(4) – C(3)	114.4(3)
C(3) – C(4)	1.406(4)	O(4) – C(4) – C(5)	125.1(3)
C(4) – C(5)	1.364(4)	C(3) – C(4) – C(5)	120.6(3)
C(5) – C(6)	1.402(5)	C(4) – C(5) – C(6)	119.7(3)
O(5) – C(6)	1.349(4)	O(5) – C(6) – C(1)	122.3(3)
-	-	O(5) – C(6) – C(5)	115.7(3)
-	-	C(1) – C(6) – C(5)	122.0(3)
-	-	O(1) – C(7) – O(2)	120.7(3)
-	-	O(1) – C(7) – C(1)	122.0(3)
-	-	O(2) – C(7) – C(1)	117.3(3)

[a] Atom numbering is as in Fig. 19.

Table 6. Bond lengths (Å) and angles (o) of **33**.

	Bisected			Eclipsed			Relative Energy
Method	E_{total}	[C=O--H-C]	[C=O--H-O]	E_{total}	[C=O--H-C]	[C=O--H-O]	
	(kcal/mol)	Å	Å	(kcal/mol)	Å	Å	(E_{eclip} -E_{bist})
X-Ray	-	2.535	1.68(4)	-	-	-	-
Ab-intio	- 470792.80	2.574	1.565	-470791.40	2.139	1.557	1.40
PM3	-2812.50	2.647	1.780	-2811.10	2.309	1.780	1.40
AM1	-2813.50	2.554	1.974	-2812.50	2.186	1.969	1.0

[a] Average of three calculations.

Table 7. Experimental and calculated[a] hydrogen bond lengths and energies (kcal/mol) for bisected and eclipsed structure of **33**.

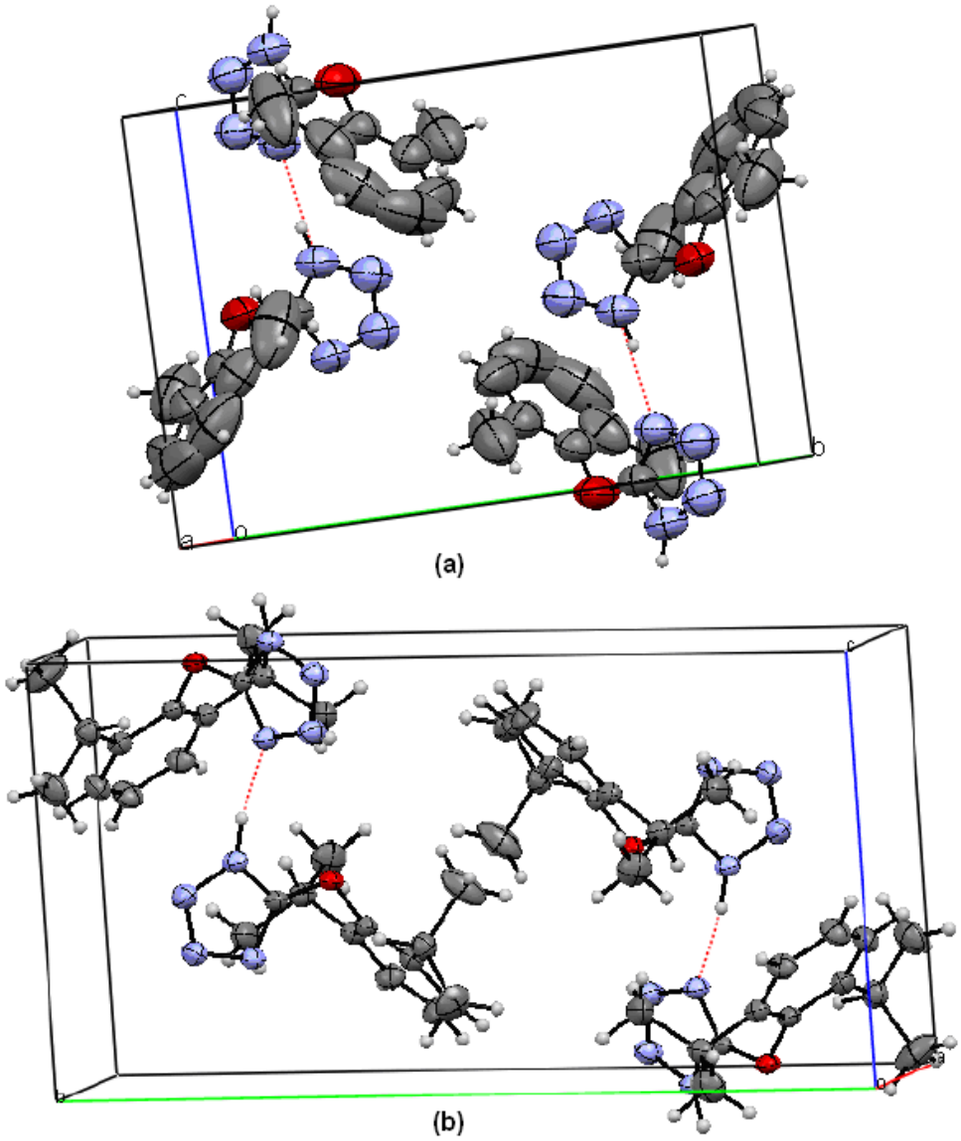

Figure 22. Crystal packing diagram of **34** (a) and **35** (b). Intermolecular hydrogen bond assigned by red dashed line (Carbon: grey; hydrogen: white; oxygen: red and nitrogen: blue).

Tetrazole ring can exist to be an equilibrium mixture of two tautomeric forms (1*H* and 2*H*-tetrazoles) "(Dabbagh & Lwowski, 2000)". 5-Aryloxy (1*H*) and/or (2*H*)-tetrazoles often show intermolecular hydrogen bond "(Noroozi Pesyan, 2011)". For instance, the crystal packing diagram of 5-(2,6-dimetylphenoxy)-(1*H*)-tetrazole (**34**) and 5-(2,6-diisopropylphenoxy)-(1*H*)-tetrazole (**35**) show intermolecular hydrogen bond (Fig. 22). In the compound **34**, the crystal structure indicated that the tetrazole and phenyl rings are nearly perpendicular to each other, forming a dihedral angle of 95.5° (*versus* 92.06° from calcd. B3LYP/6-31G(d) and 6-31+G(d)). Because of the conjugation of O1 with tetrazole ring, the bond distance C1–O1 [1.322 Å] is slightly shorter than O1–C7 [1.399 Å]. These bond distances for C1–O1 and O1–C2 were obtained 1.333 and 1.419 Å with calculation by B3LYP/6-31G(d) method, respectively and also 1.332 and 1.420 Å derived with calculation by B3LYP/6-31+G(d) basis set, respectively. These data are in good agreement with experimental results (Table 8). In the compound **35**, the crystal structure indicated that the tetrazole and phenyl rings are nearly perpendicular to each other, forming a dihedral angle of 85.91° (*versus* 107.2° from calcd. B3LYP/6-31G(d)). Because of the conjugation of O1 with tetrazole ring, the bond distance C2–O1 [1.3266(14) Å] is slightly shorter than O1–C7 [1.4257(13) Å]. These bond distances for C2–O1 and O1–C7 were obtained 1.332 and 1.423 Å with calculation by B3LYP/6-31+G(d) method, respectively and are in good agreement with experimental results. These bond distances were also obtained 1.322 and 1.422 Å with calculation by B3LYP/6-31G(d) method, respectively. The torsion angles between phenyl ring and each of methyl units on two isopropyl groups are -110.70°, 124.18° and 116.15° and 154.12°, respectively (Table 9).The selected parameters of bond length, angles and torsion angles of **34** and **35** derived by experimental and calculated results are shown in Tables 8 and 9.

The crystal packing of **34** exhibits an intermolecular N1–H1⋯N4 hydrogen bonds and comparized with the calculated at DFT (B3LYP) at 6-31G(d) and 6-31+G(d) basis sets (Table 10). The crystal structure indicated that the bond distance value between donor – hydrogen (N1–H1) and hydrogen-acceptor (H1⋯N4) were found in results 0.861 and 1.959 Å, respectively. For instance, these bond distances were also found in results 1.033 for (N1–H1) and 1.814 for (H1⋯N4) by calculated at B3LYP/6-31G(d) and 1.031 for (N1–H1) and 1.809 for (H1⋯N4) B3LYP/6-31+G(d), respectively. The donor-acceptor distance value (N1⋯N4) was obtained 2.804 by experimental method. This parameter was found 2.842 and 2.838 Å by calculated methods B3LYP/6-31G(d) and 6-31+G(d), respectively. The angle of N1-H1⋯N4 was found 169.9, 172.9 and 172.1° by experimental, calculated B3LYP/6-31G(d) and B3LYP/6-31+G(d) basis sets, respectively. The results of calculated method (specially 6-31+G(d) basis set) are in good agreement with experimental results (Table 10).

The crystal packing of **35** also exhibits an intermolecular N3–H31⋯N6 hydrogen bonds and comparized with the calculated at DFT (B3LYP) at 6-31G(d) and 6-31+G(d) basis sets (Table 10). The crystal structure indicated that the bond distance value between donor – hydrogen (N3–H) and hydrogen-acceptor (H31⋯N6) were found in results 0.926 and 1.919 Å, respectively. For instance, these bond distances were also found in results 1.03 for (N3–H31) and 1.91 for (H31⋯N6) by calculated at B3LYP/6-31G(d) and 1.01 for (N3–H) and 1.93 for

Compd. **34**			
Atom	Ex.	Calcd.[a]	Calcd.[b]
O1-C1	1.322	1.332	1.333
O1-C2	1.399	1.420	1.419
C1-N1	1.327	1.348	1.348
C1-N4	1.305	1.316	1.315
N1-N2	1.354	1.362	1.363
N1-H1	0.861	1.01	1.01
N2-N3	1.285	1.288	1.288
N3-N4	1.368	1.368	1.368
C2-C3	1.349	1.397	1.396
C2-C7	1.389	1.397	1.396
C3-C9	1.518	1.508	1.508
C7-C8	1.495	1.508	1.508
C1-O1-C2	117.3	117.6	117.6
O1-C1-N1	121.0	120.8	120.8
O1-C1-N4	129.3	130.05	130.05
C1-N1-H1	126.1	130.4	130.4
O1-C2-C3	117.8	117.8	117.8
O1-C2-C7	116.3	117.8	117.8
C2-C3-C9	120.4	121.2	121.2
C2-C7-C8	123.0	121.2	121.2
C2-O1-C1-N1	170.0	-180	-180
O1-C1-N1-H1	-0.8	0.0	0.0
O1-C2-C3-C9	4.4	4.9	4.9
O1-C2-C3-C4	-175.4	-175.6	-175.6
O1-C2-C7-C8	-5.7	-4.9	-4.9

[a] Calculated at B3LYP/6-31+G(d) basis set.
[b] Calculated at B3LYP/6-31G(d) basis set.

Table 8. The selected bond lengths (Å), angles (°) and torsion angles (ϕ) for **34**. Experimental and B3LYP/6-31+G(d) and B3LYP/6-31G(d).

(H⋯⋯N6) B3LYP/6-31+G(d), respectively. The donor-acceptor distance value (N3⋯⋯N6) was obtained 2.835 by experimental method. This parameter was found 2.941 and 2.912 Å by calculated methods B3LYP/6-31G(d) and 6-31+G(d), respectively. The angle of N3–H31⋯⋯ N6 was found 169.1, 177.0 and 173.0° by experimental, calculated B3LYP/6-31G(d) and B3LYP/6-31+G(d) basis sets, respectively. The results of calculated method (specially 6-31+G(d) basis set) are in good agreement with experimental results (Table 10). Compounds **34** (entry no. CCDC-838541) and **35** (entry no. CCDC-819010) were deposited to the Cambridge Crystallographic Data Center and are available free of charge upon request to CCDC, 12 Union Road, Cambridge, UK (Fax: +44-1223-336033, *e-mail*: *deposit@ccdc.cam.ac.uk*).

Compd. **35**			
Atom	Ex.	Calcd.[a]	Calcd.[b]
O1-C2	1.327	1.332	1.322
O1-C7	1.426	1.423	1.422
C2-N3	1.327	1.349	1.348
C2-N6	1.314	1.316	1.315
N3-N4	1.358	1.362	1.363
N3-H31	0.926	1.01	1.010
N4-N5	1.288	1.288	1.288
N5-N6	1.373	1.368	1.368
C7-C8	1.392	1.401	1.400
C7-C15	1.389	1.404	1.403
C8-C9	1.521	1.525	1.525
C15-C16	1.528	1.527	1.527
C2-O1-C7	114.49	118.64	118.39
O1-C2-N3	121.3	120.47	120.38
O1-C2-N6	128.5	130.51	130.57
C2-N3-H31	129	130.43	130.33
O1-C7-C8	116.8	118.67	118.72
O1-C7-C15	117.9	117.02	117.08
C7-C8-C9	120.8	123.14	123.08
C8-C9-H91	106.1	108.37	108.29
C10-C9-C11	111.7	111.27	111.41
C7-C15-C16	122.2	124.82	124.6
C15-C16-H161	106.3	104.94	105.01
C17-C16-C18	111.1	111.52	111.49
C7-O1-C2-N3	-174.8	178.5	178.7
O1-C2-N3-H31	-7.5	-0.2	-0.08
O1-C7-C8-C9	1.5	1.6	1.9
O1-C7-C8-C12	-176.5	-177.3	-177.3
O1-C7-C15-C16	-2.0	-1.1	-1.2
C7-C8-C9-C10	154.1	119.45	116.5
C7-C8-C9-C11	-80.2	-115.5	-118.5
C7-C15-C16-C17	-110.7	-63.8	-63.8
C7-C15-C16-C18	124.2	64.7	64.5

[a] Calculated at B3LYP/6-31+G(d) basis set.

[b] Calculated at B3LYP/6-31G(d) basis set.

Table 9. The selected bond lengths (Å), angles (°) and torsion angles (ϕ) for **35**. Experimental and B3LYP/6-31+G(d) and B3LYP/6-31G(d).

	D-H····A	D-H	H····A	D····A	D-H····A (degree, °)
Exp.[a] (**34**)	N1-H1····N4[b]	0.861	1.959	2.804	166.9
Calcd.[c] (**34**)		1.033	1.814	2.842	172.9
Calcd.[d] (**34**)		1.031	1.809	2.838	172.1
Exp.[a] (**35**)	N3-H31····N6[e]	0.926	1.919	2.835	169.1
Calcd.[c] (**35**)		1.03	1.91	2.941	177
Calcd.[d] (**35**)		1.01	1.93	2.912	174

[a] Experimental.
[b] Symmetry codes: (i) *x*, −*y*+3/2, *z*+1/2.
[c] Calculated at B3LYP/6-31G(d).
[d] Calculated at B3LYP/6-31+G(d).
[e] Symmetry codes: (i) *x*, −*y*+3/2, *z*+1/2.

Table 10. Experimental and calculated B3LYP/6-31+G(d) and B3LYP/6-31G(d) levels for hydrogen-bond geometry of **34** and **35** (Å, °)

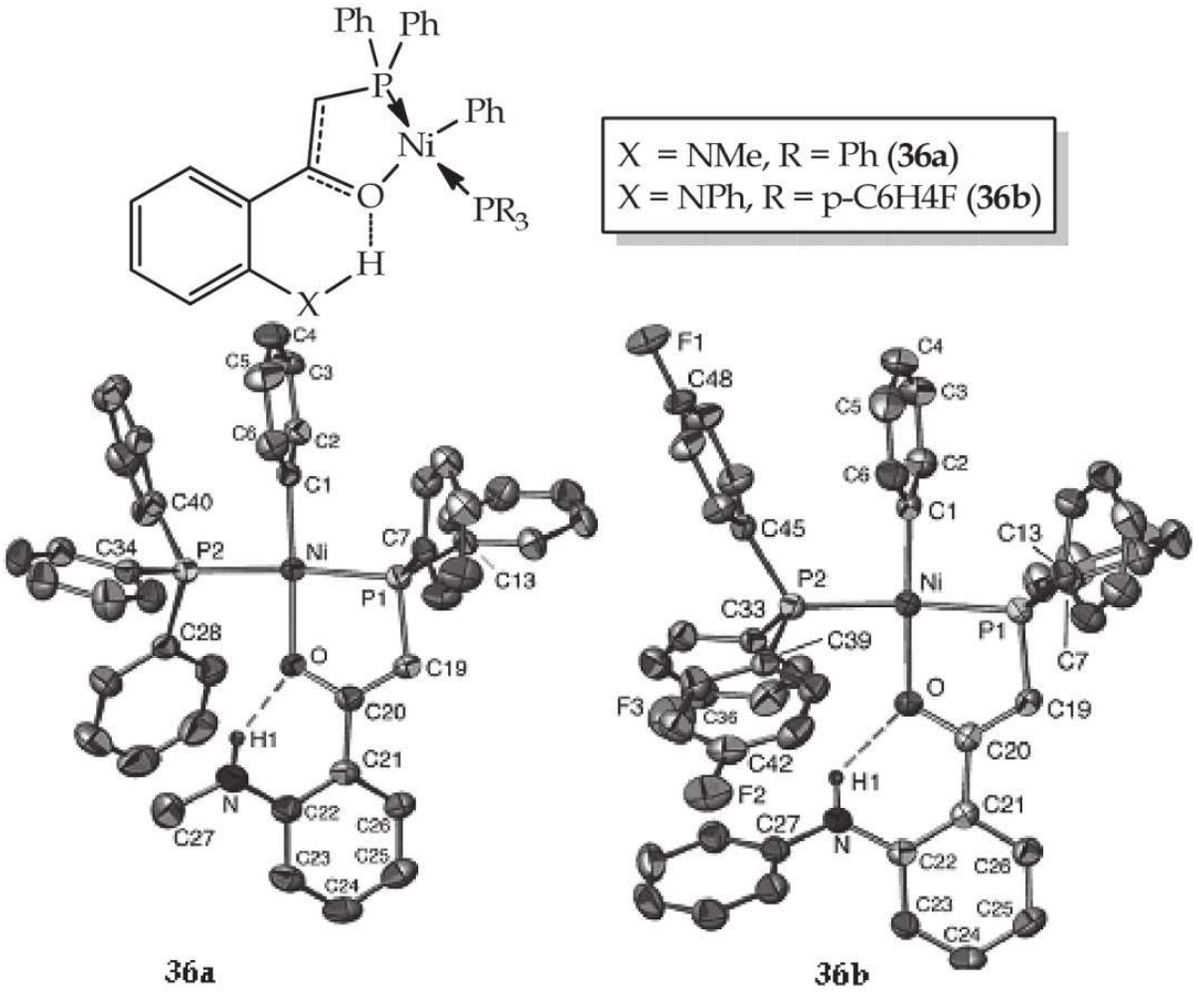

Figure 23. Formula and crystal structures of the compounds **36a** and **36b**.

Nickel(II) complexes containing specific phosphorus– oxygen chelating ligands are very efficient catalysts for the oligomerisation of ethylene to linear form "(Braunstein et al., 1994)". For instance, Nickel(II) diphenylphosphinoenolate complexes have been prepared from (*ortho*-

HX- substituted benzoylmethylene)triphenyl phosphoranes (X = NMe, NPh) and [Ni(1,5-cod)$_2$] in the presence of a tertiary phosphine (PPh_3 or P(*p*-$C_6H_4F)_3$) and their crystal structures have been studied by Braunstein et al. (structures of **36a** and **36b**). Formula and crystal structures of the compounds **36a** and **36b** are shown in Fig. 23. Crystallographic study of the complexes **36a** and **36b** establishes the presence of strong intramolecular hydrogen bonding between the enolate oxygen and the N–H functional group "(Braunstein et al., 2005)". The most notable feature in these structures is the strong intramolecular N–H···O hydrogen bonding: the calculated distance between the NH hydrogen atom and the oxygen atom of the enolate ligand is short: 2.18(5) Å in **36a** and 2.00(5) Å in **36b**, respectively "(Taylor & Kennard, 1982)".

Intramolecular hydrogen bond is also shown in alkoxyamines. These compounds and persistent nitroxide radicals are important regulators of nitroxide mediated radical polymerization (NMP). The formula and crystal structure of β-phosphorylated nitroxide radical (**37**) is shown in Fig. 24. Compound **37** show an eight-membered intramolecular hydrogen bond between P=O···H-O (versus N-O···H-O). The hydrogen bond distance for two enantiomers of **37** is different. The hydrogen bond distances of P=O···H-O in (*R*)- and (*S*)-**37** are 1.570 and 2.040 Å, respectively and favored. Instead, the hydrogen bond distance for N-O···H-O in (*R*)- and (*S*)-**37** are 3.070 and 3.000 Å, respectively and unfavored "(Acerbis et al., 2006)".

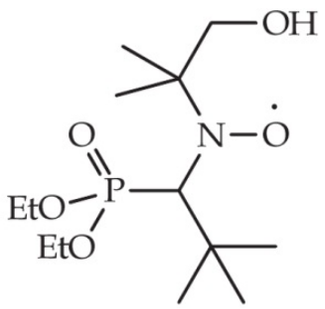

37

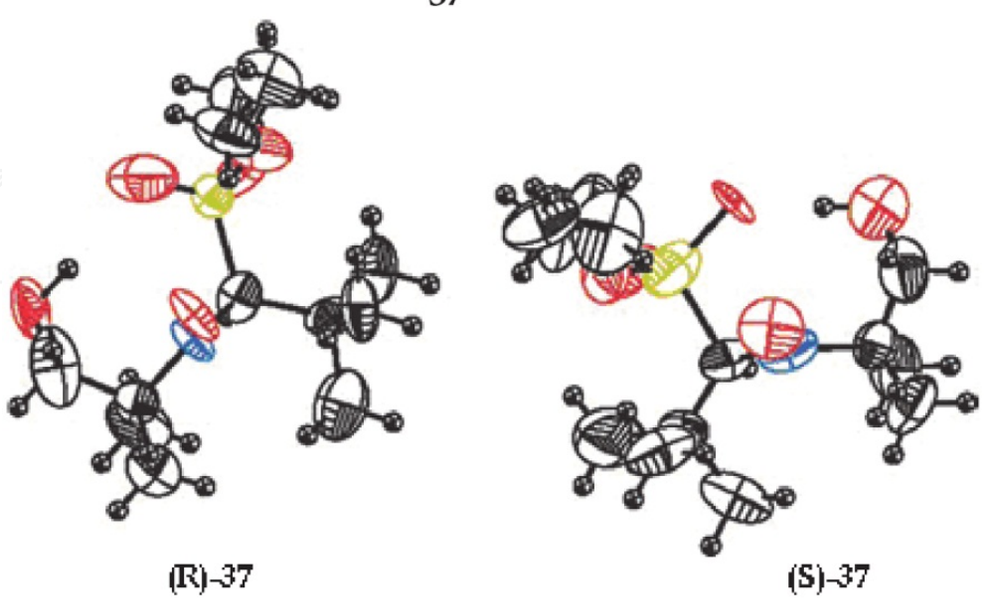

Figure 24. Formula and crystal structure of two enantiomers of compound **37** (O: red, N: blue and P: yellow).

1,8-diaminonaphthalene derivatives such as; *N*-(8-(dimethylamino)naphthalen-1-yl)-2-fluoro-*N*-methylbenzamide (**38**) is a proton sponge. An unusual strong intramolecular hydrogen bond was observed in the protonated **38**. In compound **38** in which a protonated amine group (**38-H**$^+$) can act as a donor suitably positioned to engage in a strong intramolecular hydrogen bond with the amide nitrogen atom rather than with the carbonyl oxygen atom (Scheme 9). Crystal structure of the triflate salt of **38-H**$^+$ is shown in Fig. 25. The unit cell consists of two molecules of **38-H**$^+$, two triflate counter ions, and one molecule of water. The dashed line indicates the proposed hydrogen bond between H1A and N2A. Selected bond lengths and angles are N2A–H1A = 2.17(4), N1A–N2A = 2.869(5), C14A–N2A = 1.369(5) (Å) and N2A–H1A–N1A = 136(3)° "(Cox et al., 1999)".

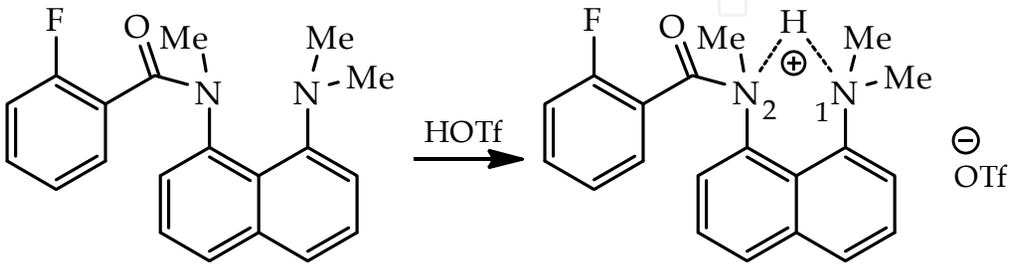

38 **38-H**$^+$

Scheme 9. Protonation of **38** in the presence of trifluoromethanesulfonic acid (TfOH).

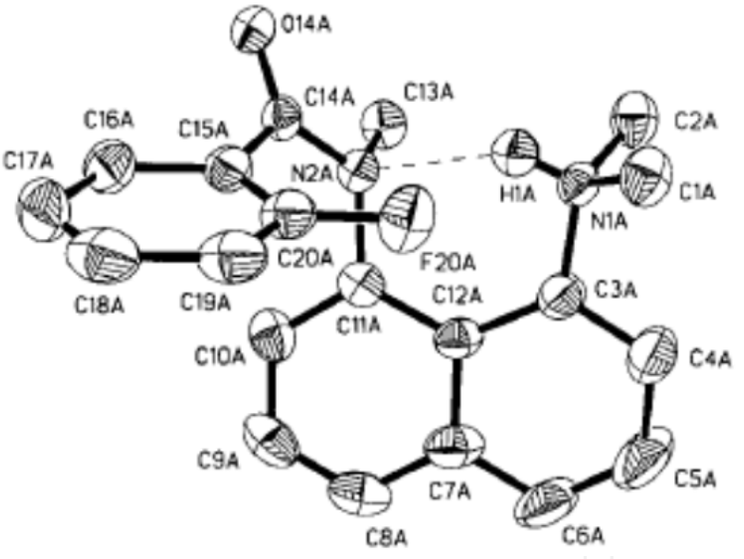

Figure 25. Crystal structure of the triflate salt of **38-H**$^+$ (50% ellipsoids and triflate counter ion is omitted).

2,4,6-Trisubstituted phenolic compounds such as 2,4,6-tri-*tert*-butyl phenol are as antioxidant "(Jeong et al., 2004)". Owing to the nature of the catalytic centres of galactose oxidase (GAO) and glyoxal oxidase (GLO), the *N*,*O*-bidentate pro-ligand, 2'-(4',6'-di-*tert*-butylhydroxyphenyl)-4,5-diphenyl imidazole (LH) (**39**) has been synthesized "(Benisvy et al., 2001)". The compound **39** possesses no readily oxidisable position (other than the phenol) and involves *o*- and *p*-substituents on the phenol ring that prevent radical coupling reactions. The compound **39** undergoes a reversible one-electron oxidation to generate the

corresponding $[LH]^{+}$ radical cation that possesses phenoxyl radical character. The unusual reversibility of the $[LH]/[LH]^{+}$ redox couple is attributed to a stabilisation of $[LH]^{+}$ by intramolecular O–H····N hydrogen bonding "(Benisvy et al., 2003)". The formula and crystal structure of **39** are shown in Fig. 26. Crystal structure of **39** shows an intra- and intermolecular hydrogen bonds in **39**. In respect of the chemical properties of **39**, there is a strong intramolecular hydrogen bond between the phenolic O–H group and N(5) of imidazole ring. The strength of this hydrogen bond, as measured by the O(1)····N(5) distance of 2.596(2) Å and the O(1)–H(1)····N(5) angle of 150.7°. Also, the N–H group of imidazole ring in **39** is involved in an intermolecular N–H····O hydrogen bond [N(2) ···· O(1S) 2.852(2) Å and N(2)–H(2A)····O(1S) 168.8°] to an adjacent trapped acetone molecule (**39·Me$_2$CO**) "(Benisvy et al., 2003)".

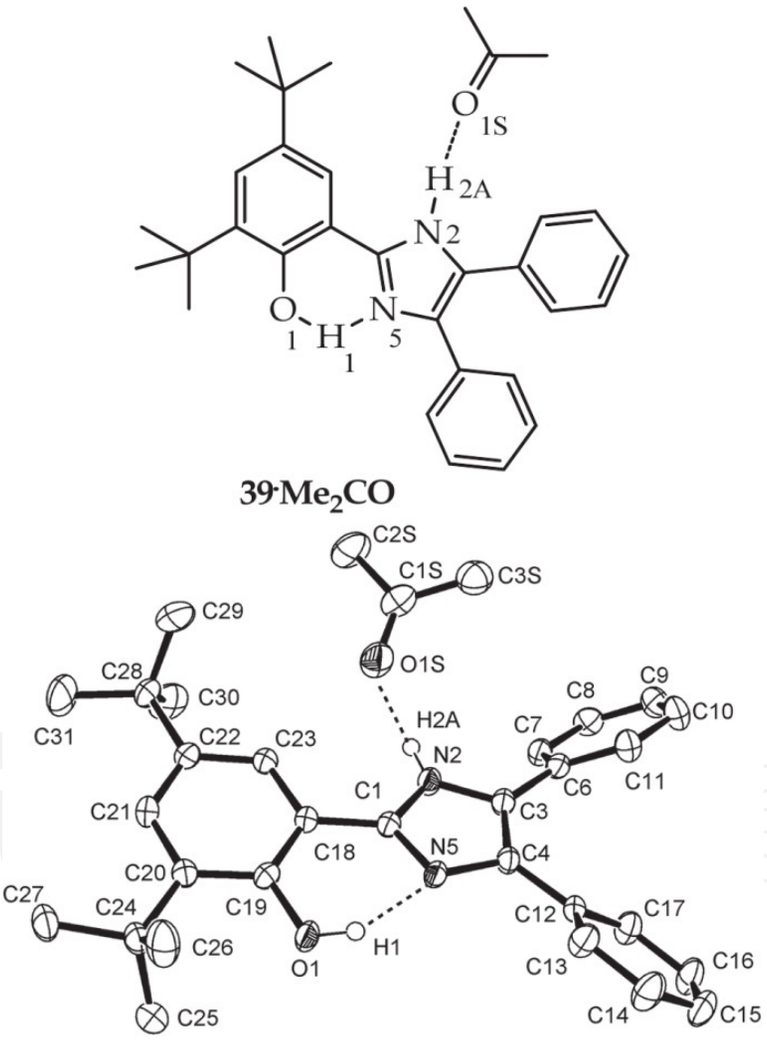

Figure 26. Formula and crystal structure of **39·Me$_2$CO**.

The azamacrocyclic ligand 1,4,7-triazacyclononane or TACN, **40**, has attracted considerable interest in recent years for its applications in oxidative catalysis. Another application of this compound was discussed by Pulacchini, et al. "(Pulacchini et al., 2003)". The incorporation of the 1,2-diaminocyclohexane moiety into a 1,4,7-triazacyclononane macrocyclic ligand was

done by this research group, as it is an inexpensive starting material and both enantiomers are readily available. Moreover, this chiral framework has been included in a number of ligands that have been successfully applied in a range of asymmetric catalytic processes by Jacobsen et al. in metallosalen complexes "(Jacobsen & Wu, 1999)".

Crystal structure of **41** is shown in Fig. 27 and revealed the structure of the macrocyclic ligand in which the six-membered ring has chair conformation (Fig. 27). The asymmetric unit is completed by the two chloride ions and a water molecule in which all C–C, C–O and C–N bonds are unexceptional. Two short hydrogen bonding interactions of 2.724(4) Å between N(1)–H(01)···O(1) and 2.884(5) between N(2)–H(05)···O(1) within the macrocycle are then supplemented by an extensive hydrogen bonding network between the ammonium nitrogen atoms N(1) and N(2) the two chloride ions Cl(1) and Cl(2), as well as the water molecule of crystallisation, as shown in Fig. 28. The roles of the two chloride ions in the network are distinct with Cl(1) acting as a direct bridge between two macrocyclic moieties as well as linking to a third *via* a water molecule. In contrast, the second chloride ion, appears to essentially serve to template the macrocyclic ligand into the conformation observed *via* hydrogen bonding interactions with N(1)–H(01) and N(2)–H(05). The second chloride ion also links to other macrocyclic moieties *via* the water molecules.

The following hydrogen bond lengths (Å) were observed from the polymeric hydrogen bonding array in **41·2HCl·H₂O**.; N(1)–H(06)···Cl(1) 3.099(4), N(1)–H(01)···Cl(2) 3.185(4), N(1)–H(01)···N(2) 3.043(5), N(1)–H(01)···O(1) 2.724(4), N(2)–H(02)···Cl(1)#1 3.103(4), N(2)–H(05)···Cl(2) 3.108(3), N(2)–H(05)···O(1) 2.884(5), O(2)– H(04)···Cl(1) 3.271(4), O(2)–H(03)···Cl(2)#2 3.217(4) "(Pulacchini, (2003)".

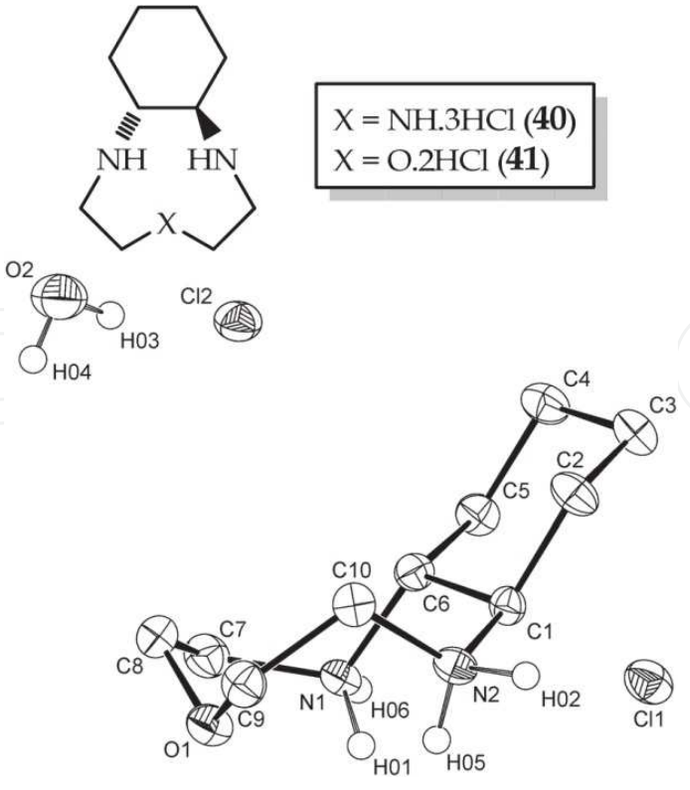

Figure 27. Formula structures of **40** and **41** and crystal structure of **41·2HCl·H₂O**.

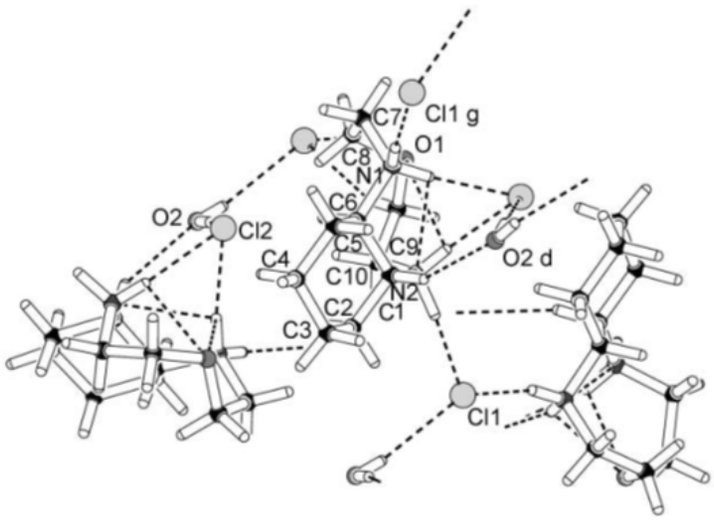

Figure 28. Polymeric hydrogen bonding network in **41·2HCl·H₂O** "(Pulacchini, (2003)".

In all thiohelicene crystals (see also Figs. 1 and 2) specific interactions were found involving sulfur "(Nakagawa et al., 1985; Yamada et al., 1981)" and hydrogen atoms at distances slightly shorter than the sum of van der Waals radii (1.80 Å for S and 1.20 Å for H). They are quite probably attractive, and, in all structures except **TH11** (hexathia-[11]-helicene **3**) they involve only atoms of terminal rings. In the case of the 5-ring system each molecule has two equivalent S···S interactions of 3.544 Å, while each **TH7** (tetrathia-[7]-helicene **1**) molecule is involved in four equivalent S···H contacts measuring 2.89 Å. All these interactions occur between enantiomeric pairs. Crystal structyre of pentathia-[9]-helicene (**TH9**, **42**) and crystal packing diagram of this compound including S···H contacts are shown in Figs. 29 and 30, respectively. For **42**, each molecule presents four equivalent S···H contacts at 2.87 Å, all with homochiral molecules giving rise to a quasi-hexagonal packing of tilted helices in planes parallel to the *ab* lattice plane. The crystal structure of **TH11** (**3**) is unusual because the asymmetric unit is formed by two complete molecules as opposed to half a molecule in all the lower racemic thiohelicenes. The packing environment of each of the two closely similar but crystallographically independent molecules, and of each of its halves, is unique: thus the *C*2 axes bisecting the central ring of each **TH11** (**3**) molecule are noncrystallographic. This situation is likely to arise in order to optimize the complex network of specific interactions involving S and H atoms. It leads to larger than expected asymmetric units and lower crystal symmetry, common occurrences in hydrogen bonded molecular systems. In the triclinic **TH11** (**3**) crystals four nonequivalent short S···S and an equal number of S···H interactions are found "(Caronna et al., 2001)". The essential geometric features of all these contacts in the racemic thiohelicene series and evidencing a remarkable consistency of the S···H interaction with expectations for weak hydrogen bonds have been reported "(Desiraju & Steiner, 2000)".

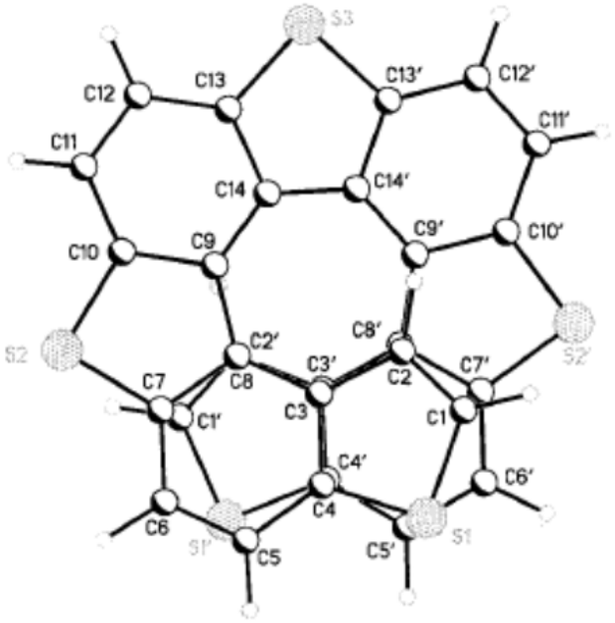

Figure 29. Crystal structure of **TH9** (**42**).

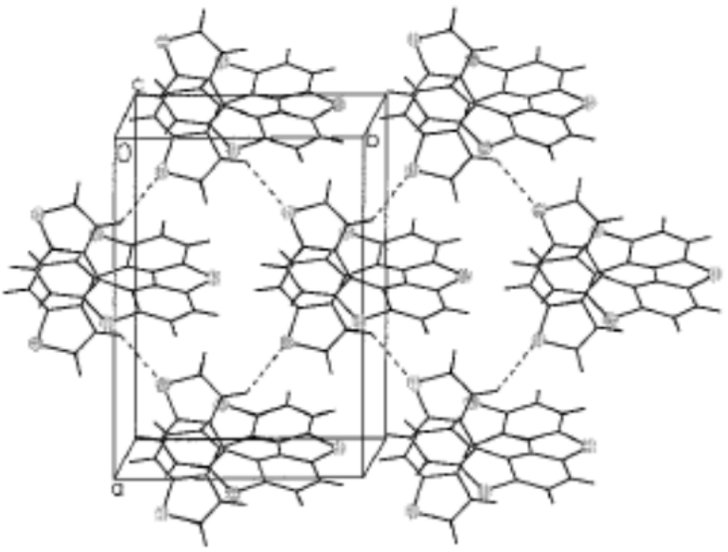

Figure 30. Crystal packing diagram of **42** in which each molecule consists of four equivalent S···H contacts.

The fused pyrimidines such as pyrimido[4,5-*c*]pyridazine-5,7(6*H*,8*H*)-diones, which are common sources for the development of new potential therapeutic agents, is well known "(Altomare et al., 1998; Brown, 1984; Hamilton, 1971)". Some of this class of compounds play new heterocyclizations based on $\left\{S_N^H\right\}$ methodology as *N*(2)-oxide and 3-alkylamino derivatives of 6,8-dimethylpyrimido[4,5-*c*]pyridazine-5,7(6*H*,8*H*)-dione "(Gulevskaya et al., 2003)".

Recently, the synthesis of 3-arylpyrimido[4,5-c]pyridazine-5,7(6*H*,8*H*)-diones (**43a–d**) and their sulfur analogs 3-aryl-7-thioxo-7,8-dihydropyrimido[4,5-c]pyridazin-5(6H)-ones **44a–d** have

been reported "(Rimaz et al., 2010)". One of the most interesting intermolecular hydrogen bond in **43a–d** have been reported by our research group "(Rimaz et al., 2010)" (Figure 31). Owing to the less solubility of **43a–d** and **44a–d**, an attempt to achieve the single crystal of these compounds for investigation of the clustered water in their crystalline structure was failed. The ^{1}H NMR spectra of **43a–d** show two broad singlets in the range of δ = 7.00–8.00 ppm that correspond to the protons of clustered water molecule in the **43a-d**. The chemical shift values of two variable protons of water in **43a–d** in ambient temperature are shown in Table 11. There are some reasons for demonstration and interpretation of this criterion. (i) One of the evidence is the mass spectra. The mass spectra of the compounds **43a–d** show not only the molecular ion fragment (M) but also the fragment of M+18. Therefore, the strength of hydrogen bond between the proton of H_2O (H_a) and oxygen atom of carbonyl group (C5=O$\cdots$ H_a–O) and also hydrogen bond between the N6–H of **43a–d** and oxygen atom of H_2O (N6–H$\cdots$ O–H_a) is considered more than that of the hydrogen bonding in the dimer form of **43a–d** (judging by the observation of the M+18 ion) (Fig. 32) "(Rimaz et al., 2010)". It seems that at least one molecule of water clustered and joined to **43** and **44** by two strong intermolecular hydrogen bonds and dissociated neither by DMSO molecules as a polar aprotic solvent nor in mass ionization chamber. Presumably, this intermolecular hydrogen bond is of quasi-covalent hydrogen bond type. There are some reports on literatures about quasi-covalent hydrogen bonds "(Dabbagh et al., 2007; Gilli et al., 1994, 2000, 2004; G. Gilli & P. Gilli, 2000; Golič et al., 1971; Madsen et al., 1999; Nelson, 2002; Steiner, 2002; Vishweshwar et al., 2004; Wilson, 2000)".

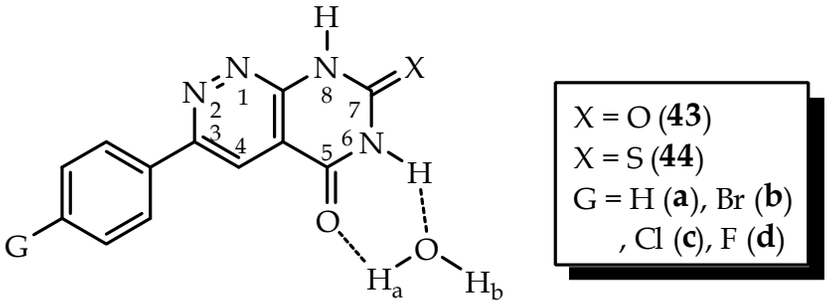

Figure 31. Formula structures of **43a–d·(H$_2$O)** and **44a–d·(H$_2$O)**.

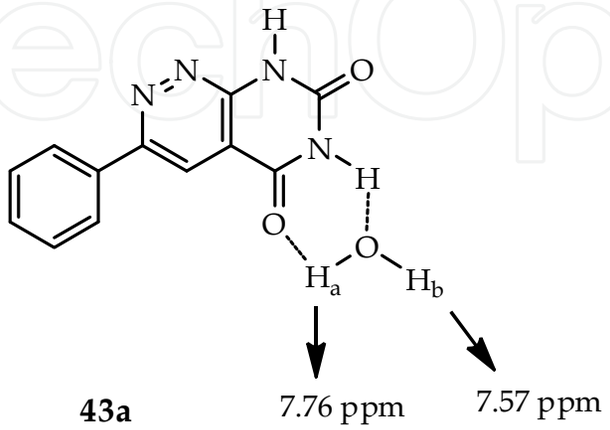

Figure 32. Representatively, strong intermolecular hydrogen bond and the chemical shifts of two hydrogen bonded protons of clustered water molecule with **43a** "(Rimaz et al., 2010)".

Compd.		δ (ppm)	
	H_a		H_b
43a	7.76		7.57
43b	7.75		7.61
43c	7.74		7.61
43d	7.75		7.61
44a		4.89	
44b		4.90	
44c		4.90	
44d		4.89	

[a] Two protons of water are equivalent in chemical shift appeared up-fielded as a broad singlet in **44a–d**.

Table 11. The chemical shift values of the two protons of a clustered water molecule in **43a–d** and **44a–d**[a] at ambient temperature "(Rimaz et al., 2010)".

The proton/deuterium exchange was examined on **43a–d** by adding one drop of D_2O. Interestingly, from hydrogen to fluorine substituent on phenyl ring in **43a–d** the exchange rate was decreased, and no deuterium exchanging of H_a and H_b was observed in **43d** while the amide protons were easily exchanged (Fig. 33). This phenomenon attributed to the fluorine atom that has made new intermolecular hydrogen bond with H_a and H_b of clustered water molecule in another molecule of **43d**. The intermolecular hydrogen bond of fluorine with the proton of clustered water (–F····H_a– and –F····H_b–) in **43d** inhibited the proton/deuterium exchanging of the clustered water protons. However, the electronegativity of fluorine atom caused deshielding of H_a and H_b on **43d** and blocked the proton/deuterium exchange (Fig. 33 and Scheme 10). Two conformational forms of **IA** and **IB** in **43d** are equivalent because of free rotation of phenyl ring about the C3–C9 and C12–F single bonds (Scheme 10) "(Rimaz et al., 2010)".

2.3. Crystal structure of some organic spiro compounds

Spiro compounds are very important and useful compounds and versatile applications. Many of heterocyclic spirobarbituric acids "(Kotha et al., 2005)", furo[2,3-*d*]pyrimidines "(Campaigne et al., 1969)" and fused uracils "(Katritzky & Rees, 1997; Naya et al., 2003)" are well known for their pharmaceutical and biological effects.

Recently, we have reported new spiro compound based on barbiturates; 5-alkyl and/or 5-aryl-1*H,* 1′*H*-spiro[furo[2,3-*d*]pyrimidine-6,5′-pyrimidine]2,2′,4,4′,6′*(*3*H,* 3′*H,* 5*H)*-pentaones which are dimeric forms of barbiturate (uracil and thiouracil derivatives) "(Jalilzadeh et al., 2011)". Reaction of 1,3-dimethyl barbituric acid (DMBA) with cyanogen bromide (BrCN) and acetaldehyde in the presence of triethylamine afforded 1,1′,3,3′,5-pentamethyl-1*H*,1′*H*-spiro[furo[2,3-*d*]pyrimidine-6,5′-pyrimidine]-2,2′,4,4′,6′(3*H*,3′*H*,5*H*)-pentaone (**46**) in excellent yield "(Jalilzadeh et al., 2011)". The formula structures of spiro compounds derived from barbituric acid (BA, **45**), DMBA **46** and 1,3-thiobarbituric acid (TBA, **47**) is shown in Fig. 34. Attempt for single crystallization of spiro compounds **45** and **47** were unsuccessful. The crystal structure and crystal packing diagram of **46** are shown in Figs. 35 and 36. This compound was crystalized in triclinic system. Selected crystallographic data for **46** is summarized at Table 12.

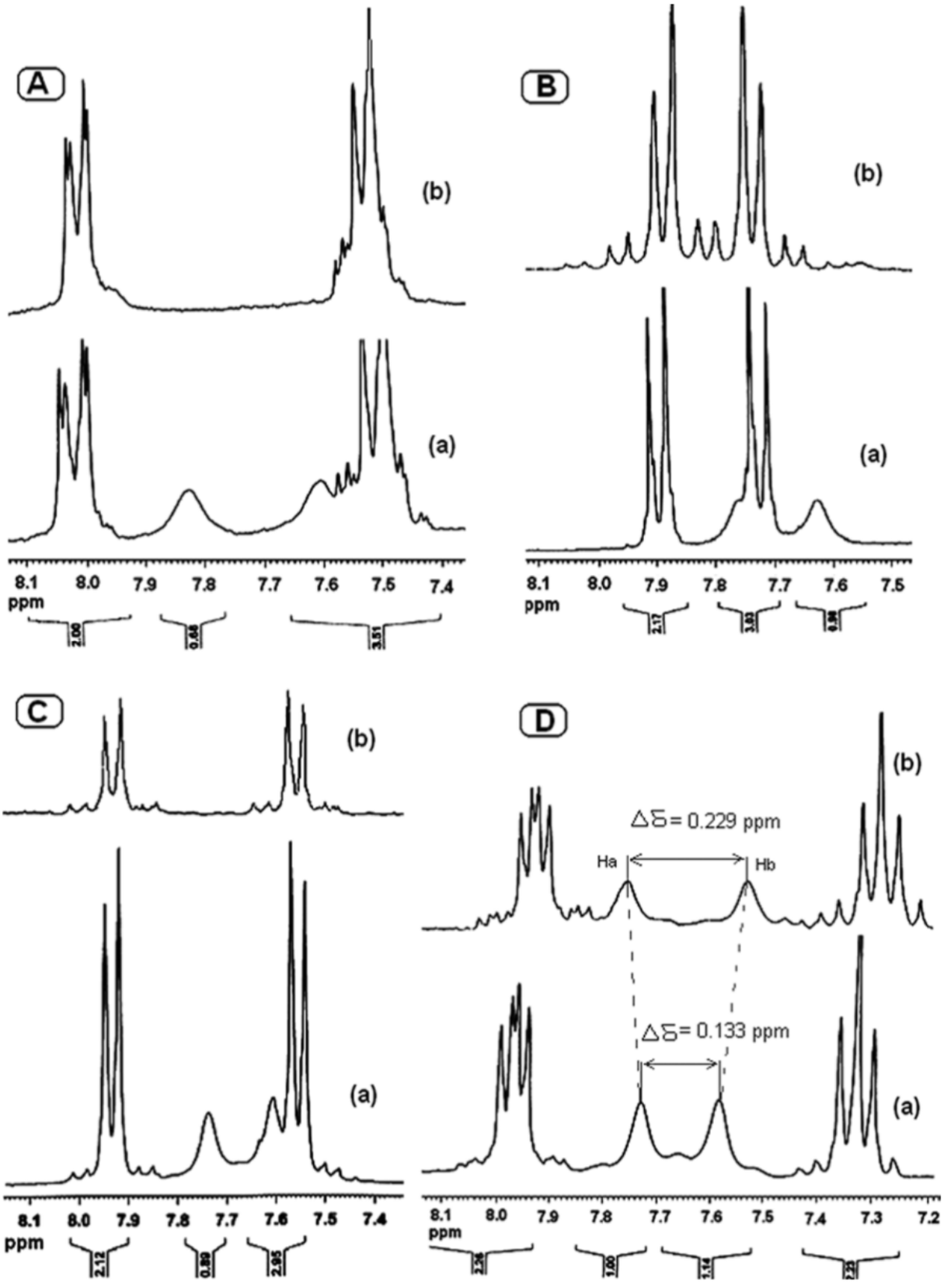

Figure 33. Proton/deuterium exchangeability of the H_a and H_b of clustered H_2O molecule in ^1H NMR spectra of **43a** (A), **43b** (B), **43c** (C) and **43d** (D). The assigned spectra are shown before (a) and after added D_2O (b). No exchange occurred in **43d** of clustered H_2O protons (D) "(Rimaz et al., 2010)".

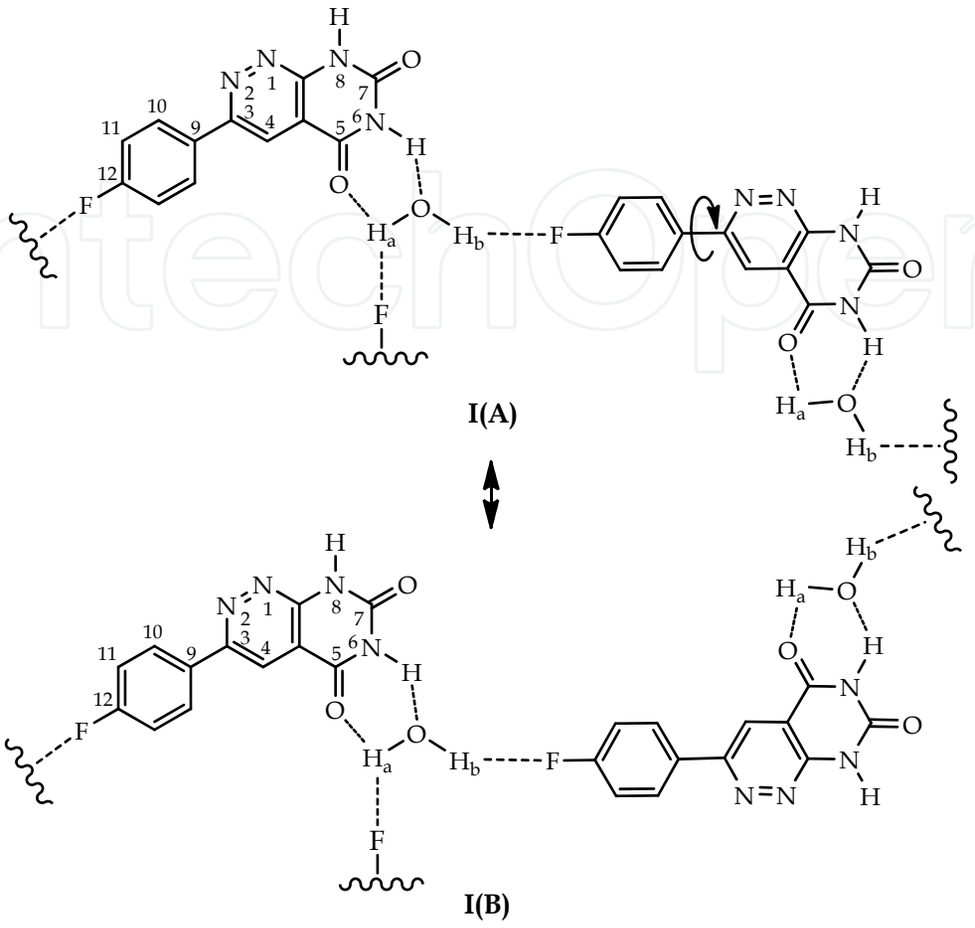

Scheme 10. Possible various types of intermolecular hydrogen bond of fluorine with a proton of a clustered were (-F····H_b- and -F····H_a-) in **43d**. This phenomenon presumably inhibited the proton/deuterium exchangeability of the clustered water protons.

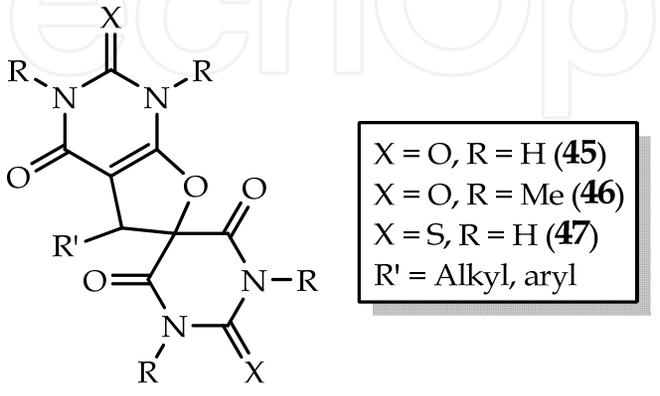

Figure 34. Formula structures of **45-47**.

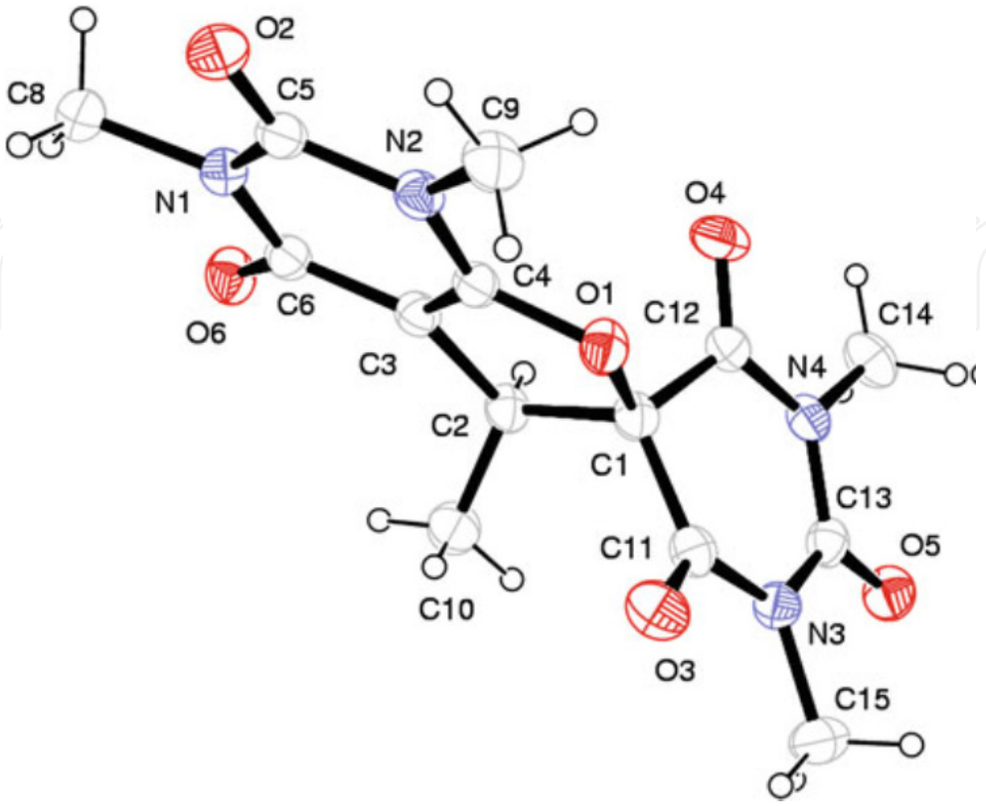

Figure 35. Crystal structure of **46.**

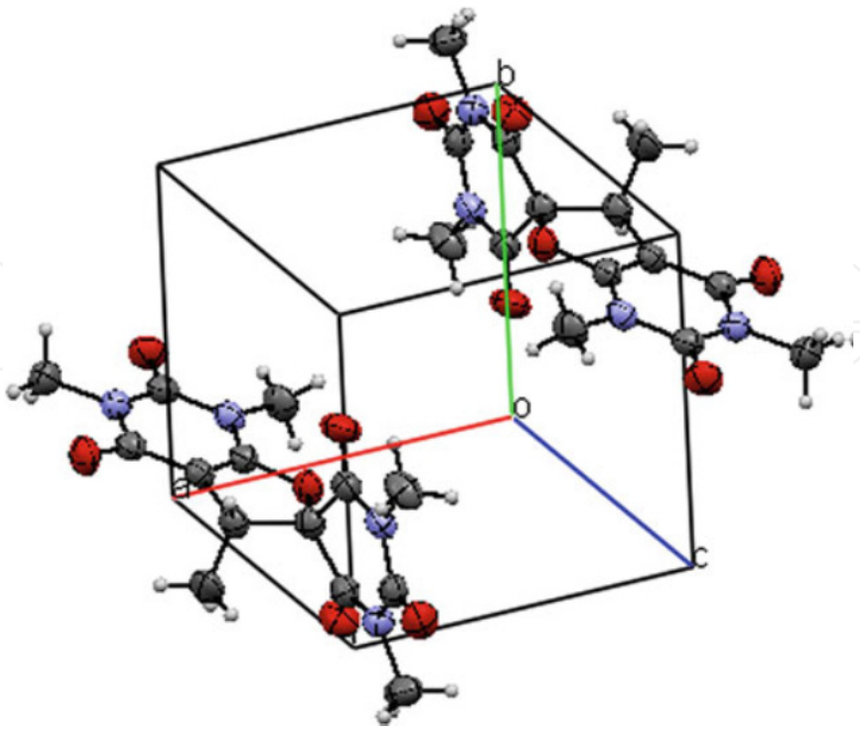

Figure 36. Crystal packing diagram of **46.**

Crystal data	
Emprical formula	$C_{14}H_{16}N_4O_6$
M	336.30
T	298 K
a (Å)	8.974 (5)
b (Å)	9.539 (5)
c (Å)	10.314 (5)
α (◦)	64.782 (5)
β (◦)	69.349 (5)
γ (◦)	69.349 (5)
V (Å3)	725.8 (7)
Z	2
F(000)	352
Dx (mg m−3)	1.539
λ (Å)	0.71073
μ(mm−1)	0.12
Data collection	
*R*int	0.062
*θ*max	29.0 ◦
*θ*min	2.3 ◦
Refinement	
R[*F*2 > 2*σ*(*F*2)]	0.067
wR(*F*2)	0.203
S	1.04

Table 12. Selected crystallographic data for **46**.

Another spiro barbiturate compound derived from the reaction of DMBA with BrCN and acetone in the presence of triethylamine is 1,1′,3,3′,5,5′-Hexamethylspiro[furo-[2,3-*d*]pyrimidine-6(5*H*),5′-pyrimidine]-2,2′,4,4′,6′(1*H*,3*H*,1′*H*,3′*H*,5*H*)-pentaone (**48**) "(Noroozi Pesyan et al., 2009)". Reaction of aldehydes with (thio)barbiturates is faster than ketones due to the reactivity and less hindrance in aldehydes. The formula and crystal structure of **48** is shown in Figs. 37 and 38, respectively. In Fig. 38, the fused 2,3-dihydrofurane ring has an envaloped conformation, and spiro pyrimidine ring has a half-chair conformation. Spiro pyrimidine ring is nearly perpendicular to 2,3-dihydro furan ring moiety as was observed earlier in the related compound. Torsion angles C2-C1-O4-C7 and C2-C1-C5-C6 are -99.39(3)° and 94.87(3) °, respectively. In the crystal, short intermolecular interaction O⋯C contacts between the carbonyl groups prove an existing of electrostatic interactions, which link the molecules into corrugated sheets parallel to *ab* plane (Table 13).

C8⋯⋯O2^{i}	2.835 (4)	C3⋯⋯O5^{ii}	2.868 (4)

Symmetry codes: (i) -x + 1, y -1/2, -z +3/2; (ii) x+1, y, z

Table 13. Selected interatomic distances (Å) in **48**.

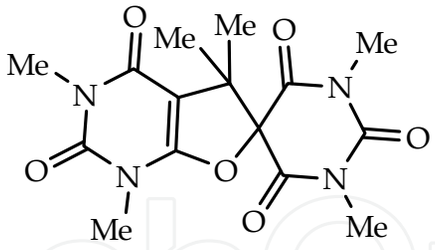

Figure 37. Formula structure of **48**.

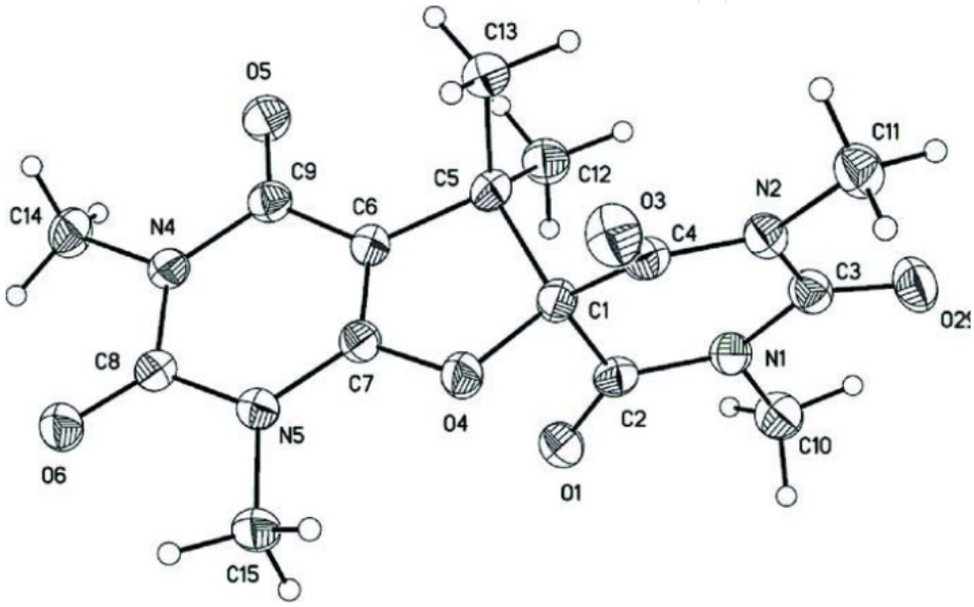

Figure 38. Crystal structure of **48**.

One of another interesting spiro barbiturate compound is the trimeric form of 1,3- DMBA; 5,6-dihydro - 1,3-dimethyl - 5,6 – bis - [l′,3′-dimethyl-2′,4′,6′-trioxo-pyrimid(5′,5′)yl]furo[2,3-*d*]uracil (**49**). This compound was first reported by electrochemical method "(Kato et al., 1974; Kato & Dryhurst, 1975; Poling & van der Helm, 1976)" and it has been reported the synthesis of **49** by chemical method for a first time two years ago "(Hosseini et al., 2011)". The formula and crystal structures of **49** are shown in Figs. 39 and 40, respectively. Crystals of **49** were obtained by slow evaporation of a solution of **49** in acetone at room temperature. The data were acquired using a STOE IPDS II diffractometer, data collection and cell refinement were processed using STOE X-AREA "(Stoe & Cie, 2002)" and data reduction was processed using STOE X-RED "(Stoe & Cie, 2002)" program. Program(s) used to refine structure was *SHELXL97* "(Sheldrick, 1997). Crystal data for **49**: Orthorhombic; $C_{18}H_{18}N_6O_9$; M = 462.38; Unit cell parameters at 293(2) K: a = 13.2422(4), b = 15.9176(6), c = 19.5817(6) Å; $\alpha = \beta = \gamma = 90°$; V = 4127.5(2) Å^3; Z = 8; μ = 0.122 mm^{-1}; Total reflection number 4275; 304 parameters; λ = 0.71073 Å; 2916 reflections with $I > 2\sigma(I)$; R_{int} = 0.056; θ_{max} = 26.49°; $R[F2 > 2\ \sigma(F2)]$ = 0.048; $wR(F2)$ = 0.112; S = 1.02, F_{000} = 1920 "(Hosseini et al., 2011)".

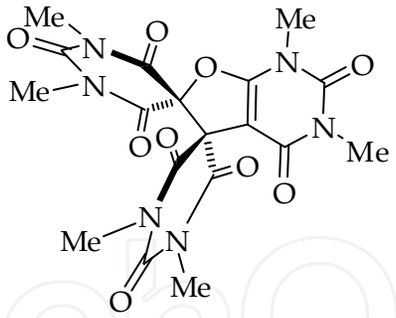

Figure 39. Formula structure of **49**.

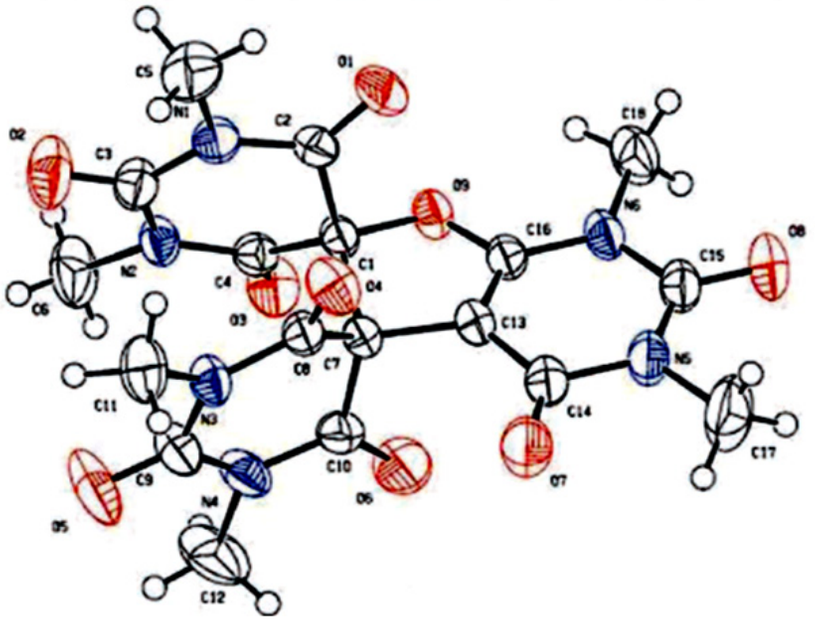

Figure 40. Crystal structure of **49**.

Amino acids derived from sugar are of extensive family of peptidomimetics "(Baron et al., 2004; Chakraborty et al., 2004)", an important sub-class of which incorporate an α-amino acid with a carbohydrate has anomeric effect. Such sugar amino acids may form spiro derivatives, some of which have been demonstrated to possess significant biological activity. For instance, the formula and crystal structure of (2'*S*,3a*R*,6*S*,6a*R*)-2,2,6-trimethyldihydro-3a*H*-spiro[furo[3,4-*d*][1,3]dioxole-4,2'-piperazine]-3',6'-dione (**50**) are shown in Figs. 41 and 42 "(Watkin et al., 2004)". This molecule show hydrogen bonds between N-H….O=C groups and are shown in crystal packing diagram, viewed along the *c* axis as dashed lines (Fig. 43).

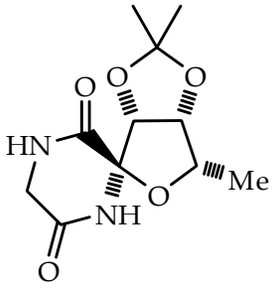

Figure 41. Formula structure of compound **50**.

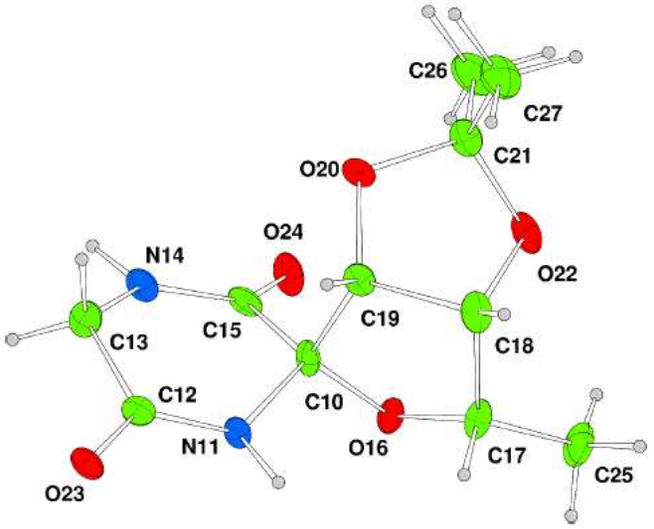

Figure 42. Crystal structure of compound **50** (Green: C, blue: N and red: O atom).

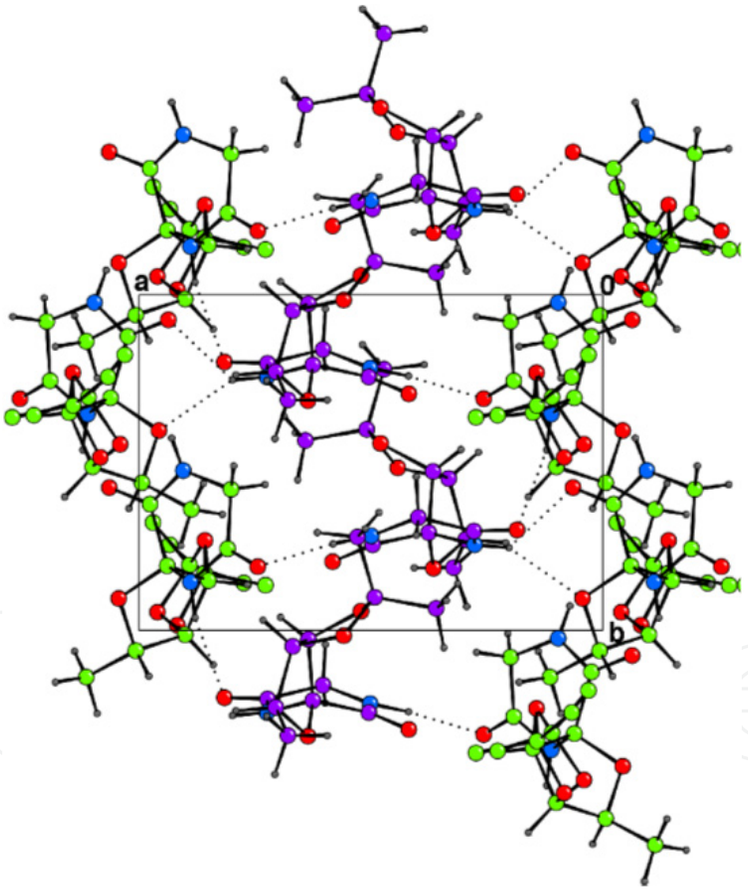

Figure 43. Crystal packing diagram of **50**.

Another interesting spiro linked barbituric acid to the cyclopentane ring moiety (spiro-nucleoside) possessing of hydroxyl and hydroxymethyl groups is (3*S*,2*R*)-3-hydroxy-2-hydroxymethyl-7,9-diazaspiro[4.5]decane-6,8,10-trione (**51**) (Figs. 44 and 45). Crystal structure of **51** shows *trans* stereochemical relationship of the two substituents hydroxyl and hydroxymethyl on cyclopentane ring moiety. The barbituric acid ring is almost planar, while

the cyclopentane moiety adopts the C3'-*endo*-type conformation. Molecules of **51** interconnected by a two-dimensional network of hydrogen bonds build layers parallel to the *ab* plane. The hydrogen bond data for **51** is outlined at Table 14 "(Averbuch-Pouchot et al., 2002)".

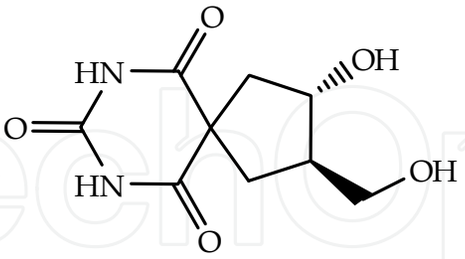

Figure 44. Formula structure of **51**.

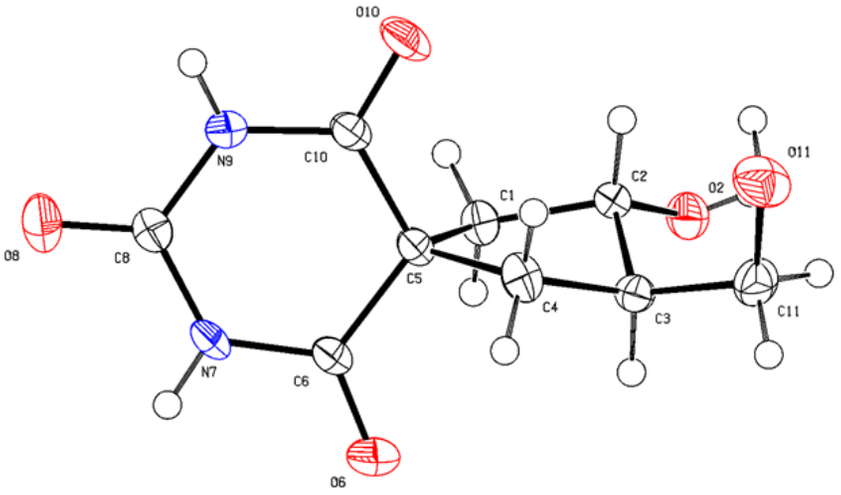

Figure 45. Crystal structure of **51**.

D—H···A	D—H	H···A	D···A	D—H···A
O11—H12···O6^{v}	0.81	2.00	2.809 (2)	173
N7—H8···O10^{iv}	0.86	1.99	2.840 (2)	170
N9—H9···O2^{vii}	0.85	2.04	2.8620 (10)	161

Symmetry codes: (iv) *x*, *y*–1, *z*; (v) *x*, *y*+1, *z*; (vii) *x*–1, *y*, *z*.

Table 14. Hydrogen-bond geometry in **51** (Å, º).

Hydantoins are very useful compounds due to their pharmaceutical behaviour such as; antitumor "(Kumar et al., 2009)", anticonvulsant "(Sadarangani et al., 2012)" and antidiabetic activity "(Hussain et al., 2009)". In the molecules of **52** and **53** (Figs. 46 and 47), the atoms in the hydantoin ring are coplanar. The crystal structures of **52** and **53** are stabilized by intermolecular N—H···O=C hydrogen bonds. The hydrogen bond lengthes and angles for **52** and **53** are summarized at Table 15. Crystal packing diagram of these molecules show the molecules are centrosymmetric dimer forms. The dihedral angle subtended by the 4-chloro- and 4-bromophenyl groups with the plane passing through the hydantoin unit are 82.98(4)° and 83.29(5)°, respectively. The cyclohexyl ring in both molecules adopts an ideal chair conformation and methyl group in an equatorial position "(Kashif et al., 2009)".

	D—H···A	D—H	H···A	D···A	D—H···A
52	N2—H2···O4^{i}	0.84 (2)	2.04 (2)	2.8763 (15)	171.5 (19)
53	N2—H2···O4^{i}	0.82 (3)	2.06 (3)	2.871 (2)	171 (3)

Symmetry code: (i) -x + 1;-y + 1;-z + 1.

Table 15. Hydrogen-bond geometry in **52** (Å, º).

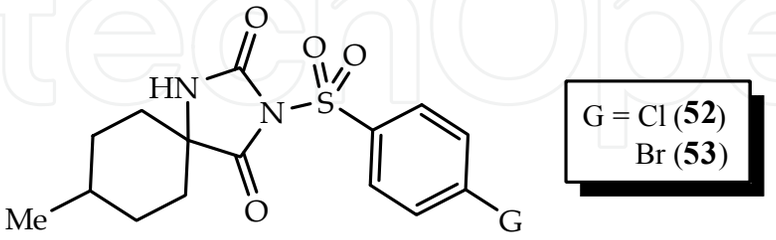

Figure 46. Formula structures of **52** and **53**.

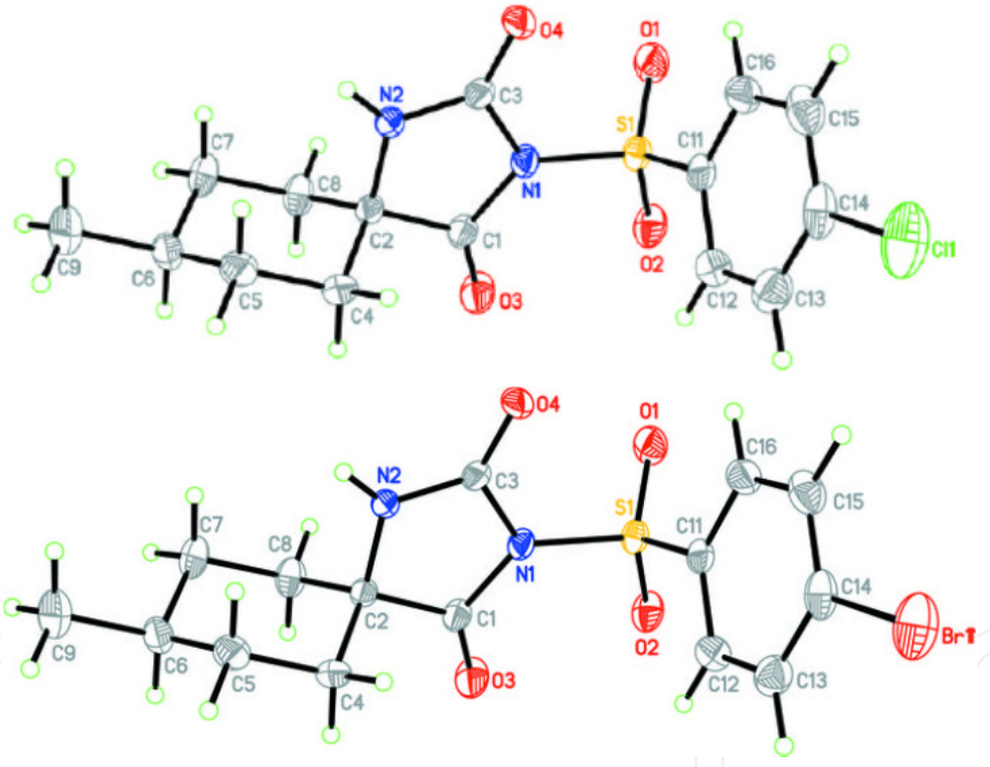

Figure 47. Crystal structures of **52** (top) and **53** (bottom).

Dihydropyridine are interesting and important systems because of their exceptional properties as calcium channel antagonists "(Si et al., 2006)" and as powerful arteriolar vasodilators "(Kiowski et al., 1990)". 4',4'-Dimethyl-2-methylsulfanyl-3,4,5,6,7,8-hexahydropyrido-[2,3-*d*]pyrimidine-6-spiro-1'-cyclohexane-2',4,6'-trione, (**54**), has a markedly polarized molecular electronic structure, and the molecules are linked into a three-dimensional framework by a combination of N–H···O, C–H···O and C–H···π hydrogen bonds (Table 16). Two independent N–H···O hydrogen bonds generate a one-

dimensional substructure in the form of a chain of rings; these chains are linked into sheets by the C–H···O hydrogen bonds, and the sheets are linked by C–H···π hydrogen bonds. Crystal packing diagram of **54** show four types of centrosymmetric ring. "(Low et al., 2004)" (Fig. 48). Compound **54** can exist in two zwitterionic forms of **54I** and **54II** (Scheme 11). For example, the bond lengths of N3–C4 and C4–O4 are both long for their types, the C4–C4A and C4A–C8A bonds are too similar in length to be characterized as single and double bonds, respectively. Also, the C8A–N8 bond, involving a three-coordinate N atom, is much shorter than the C8A–N1 bond, which involves a two-coordinate N atom. These observations, taken together, effectively preclude the polarized form (**54I**) as an effective contributor to the overall molecular electronic structure, instead pointing to the importance of the polarized vinylogous amide form (**54II**) "(Low et al., 2004)".

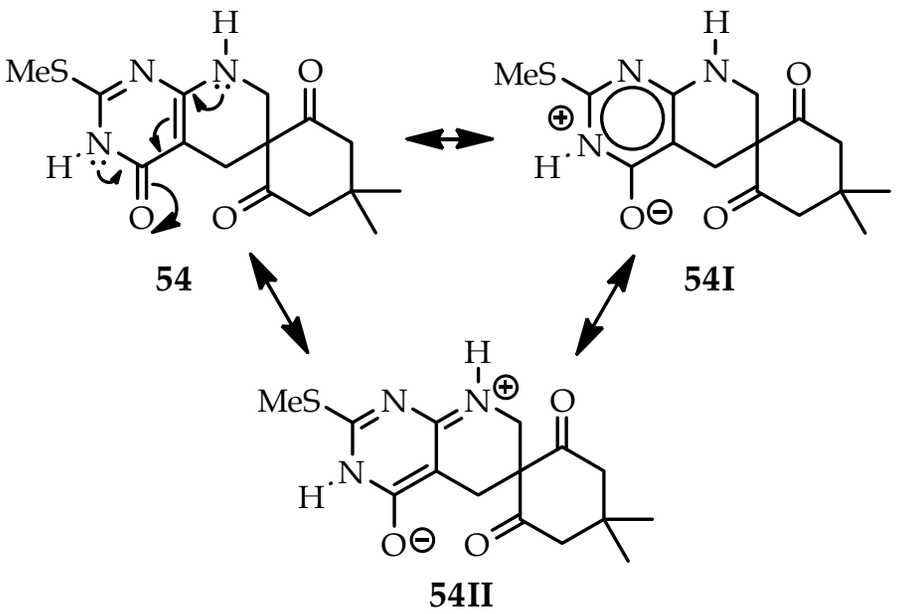

Scheme 11. Zwitterionic forms of **54**.

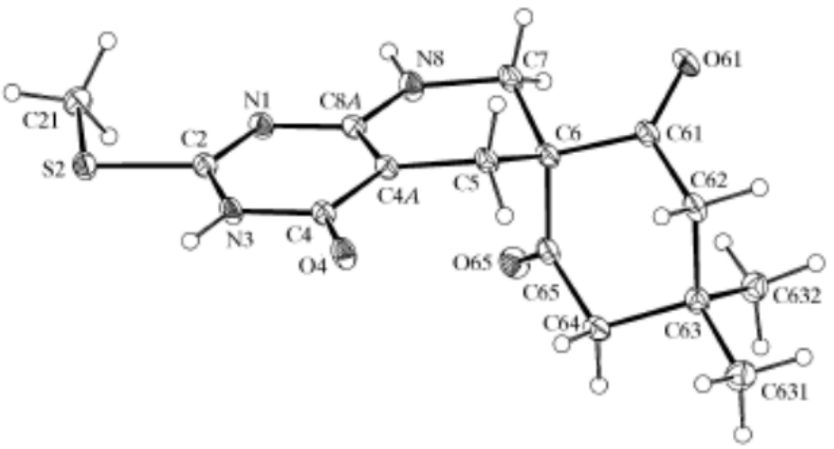

Figure 48. Crystal structure of **54**.

D–H····A	D–H	H····A	D····A	D–H····A
N3–H3····O4^{i}	0.88	1.84	2.715 (2)	176
N8–H8····O65^{ii}	0.88	2.10	2.965 (2)	166
C5–H5B....O61^{iii}	0.99	2.46	3.389 (2)	155
C64–H64A....Cg1^{iv}	0.99	2.87	3.854 (2)	173

Symmetry codes: (i) 1 - x; 1 - y; 1 - z; (ii) -x; 1 - y; -z; (iii) -x; 2 - y;-z; (iv) 1 -x;-y;-z.
Cg1 is the centroid of the pyrimidinone ring.

Table 16. Hydrogen-bonding geometry (Å, °) for **54**.

3. Conclusion

In summary, X-ray single crystal diffraction analysis of the some helicenes and other helix molecules were discussed. In continuation, the crystal structure of some organic and organometallic compounds consists of intra- and/or intermolecular hydrogen bond were described. Finally, crystal structures of some new spiro compounds were analyzed.

Author details

Nader Noroozi Pesyan
Urmia University, Iran

Acknowledgement

The author gratefully acknowledge financial support by Research Council of Urmia University

4. References

Acerbis, S; Bertin, D; Boutevin, B; Gigmes, D; Lacroix-Desmazes, P; Le Mercier, C; Lutz, J-F; Marque, SRA; Siri, D & Tordo, P (2006). Intramolecular Hydrogen Bonding: The Case of β-Phosphorylated Nitroxide (=Aminoxyl) Radical, *Helve. Chim. Acta*, 89, 2119.

Altomare, C; Cellamare, S; Summo, L; Catto, M; Carotti, A; Thull, U; Carrupt, P-A; Testa, B & Stoeckli-Evans, H (1998). Inhibition of Monoamine Oxidase-B by Condensed Pyridazines and Pyrimidines: Effects of Lipophilicity and Structure-Activity Relationships, *J. Med. Chem.*, 41, 3812-3820.

Arai, S & Hida, M In *Adv. Heterocycl. Chem.*; Katritzky, AR, Ed.; Academic: San Diego, 1992; Vol. 55, p 261.

Averbuch-Pouchot, M-T; Durif, A; Renard, A; Kottera, M & Lhomme, J (2002). (3*S*,2*R*)-3-Hydroxy-2-hydroxymethyl-7,9-diazaspiro[4.5]decane-6,8,10-trione, *Acta Cryst.*, E58, o256-o258.

Azumaya, I; Uchida, D; Kato, T; Yokoyama, A; Tanatani, A; Takayanagi, H & Yokozawa, T (2004). Absolute Helical Arrangement of Stacked Benzene Rings: Heterogeneous

Double-Helical Interaction Comprising a Hydrogen-Bonding Belt and an Offset Parallel Aromatic–Aromatic-Interaction Array, *Angew. Chem. Int. Ed.* 43, 1360-1363.

Baron, R; Bakowies, D & van Gunsteren, WF (2004). Carbopeptoid Folding: Effects of Stereochemistry, Chain Length, and Solvent, *Angew. Chem. Int. Ed.*, 43, 4055-4059. doi:10.1002/anie.200454114

Benisvy, L; Blake, AJ; Collison, D; Davies, ES; Garner, CD; McInnes, EJL; McMaster, J; Whittaker, G & Wilson, C (2003). A Phenol–imidazole Pro-ligand That Can Exist as a Phenoxyl Radical, Alone and When Complexed to Copper(II) and Zinc(II), *Dalton Trans.*, 1975.

Benisvy, L; Blake, AJ; Davies, ES; Garner, CD; McMaster, J; Wilson, C; Collinson, D.; McInnes, EJL & Whittaker, G; (2001). A Phenoxyl Radical Complex of Copper(II), *Chem. Commun.*, 1824.

Bossi, A; Falciola, L; Graiff, C; Maiorana, S; Rigamonti, C; Tiripicchio, A; Licandro, E & Mussini, PR (2009). Electrochemical Activity of Thiahelicenes: Structure Effects and Electrooligomerization Ability, *Electrochimica Acta* 54 5083.

Bragg, WH (1925). The Investigation of Thin Films by Means of X-rays, *Nature*, 115, 266-269. doi:10.1038/115266a0

Braunstein, P; Chauvin, Y; Mercier, S; Saussine, L; DeCian, A & Fischer, J (1994). Intramolecular O–H···O–Ni and N–H···O–Ni Hydrogen Bonding in Nickel Diphenylphosphinoenolate Phenyl Complexes: Role in Catalytic Ethene Oligomerisation; Crystal Structure of [NiPH{Ph_2PCH···C(···O)(*o*-C_6H_4NHPh)}(PPh_3)], *J. Chem. Soc., Chem. Commun.*, 2203. doi: 10.1039/C39940002203

Braunstein,P; Chauvin, Y; Mercier, S & Saussine, L (2005). Influence of Intramolecular N–H···O–Ni Hydrogen Bonding in Nickel(II) Diphenylphosphinoenolate Phenyl Complexes on the Catalytic Oligomerization of Ethylene, *C. R. Chimie*, 8, 31.

Brown, DJ (1984). In *Comprehensive Heterocyclic Chemistry*, vol. 3, (Eds: Katritzky, AR; Rees, CW), Pergamon Press: Oxford, pp 57.

Campaigne, E; Ellis, RL; Bradford, M & Ho, J (1969). Synthesis of Some Ureidodihydrofurans and Related Pyrimidones as Potential Antimalarials, *J. Med. Chem.* 12, 339.

Caronna, T; Catellani, M; Luzzati, S; Malpezzi, L; Meille, SV; Mele, A; Richter, C & Sinisi, R (2001). Molecular Crystal Architecture and Optical Properties of a Thiohelicenes Series Containing 5, 7, 9, and 11 Rings Prepared via Photochemical Synthesis, *Chem. Mater.* 13, 3906.

Casado, J; Patchkovskii, S; Zgierski, MZ; Hermosilla, L; Sieiro, C; Oliva, MM & Navarette, JTL (2008). Raman Detection of "Ambiguous" Conjugated Biradicals: Rapid Thermal Singlet-to-Triplet Intersystem Crossing in an Extended Viologen, *Angew. Chem., Int. Ed.*, 47, 1443.

Caspari, WA (1928). Crystallography of the Aliphatic Dicarboxylic Acids, *J. Chem. Soc. (London)*, 3235-3241.

Chakraborty, TK; Srinivasu, P; Tapadar, S & Mohan, BK (2004). Sugar Amino Acids and Related Molecules: Some Recent Developments, *Indian J. Chem. Sci.*, 116, 187-207.

Clays, K; Wostyn, K; Persoons, A; Maiorana, S; Papagni, A; Daul, CA & Weber, V (2003). Experimental Study of the Second-Order Non-linear Optical Properties of Tetrathia-[7]-helicene, *Chem. Phys. Lett.* 372, 438–442.

Collins, SK & Vachon, MP (2006). Unlocking the Potential of Thiaheterohelicenes: Chemical Synthesis as the Key, *Org. Biomol. Chem.* 4, 2518.

Corbridge, DEC (1990). *Phosphorous: An outline of it s chemistry, biochemistry and technology*. 4th ed., Elsevier, Amsterdam, Chapt. 14.

Cox, C; Wack, H & Lectka, T (1999). Strong Hydrogen Bonding to the Amide Nitrogen Atom in an "Amide Proton Sponge": Consequences for Structure and Reactivity, *Angew. Chem. Int. Ed.*, 38, 798. doi:10.1002/(SICI)1521-3773(19990315)38:6<798::AID-ANIE798>3.0.CO;2-W

Dabbagh, AH; Noroozi Pesyan, N; Najafi, CA; Brian, OP & Brian, RJ (2007). Diastereoselective Formation of 18-Membered Ring BINOL-hydrogenphosphonate Dimers-Quasi-covalent Hydrogen Bonds?, *Canadian J. Chem.*, 85, 466-474.

Dabbagh, HA & Lwowski, W (2000). Equilibria of the 5-Substituted-1,2-acylated Tetrazoles and Imidoyl Azides, *J. Org. Chem.*, 65, 7284-7290.

Dabbagh, HA; Noroozi-Pesyan, N; Patrick, BO & James, BR (2004). A One Pot Synthesis, and X-Ray Crystallographic and Computational Analyses of Methyl-2,4-dimethoxysalicylate — a Potential Anti-tumor Agent, *Can. J. Chem.*, 82, 1179.

Davies, C; Langler, RF; Krishnamohan, CV & Zaworotko, MJ (1997). A Supramolecular Carpet Formed via Self-assembly of Bis(4,4′-dihydroxyphenyl) sulfone, *Chem. Commun.*, 567.

de Broglie, M & Trillat, JJ (1925). Sur L'interprétation Physique Des Spectres X D'acides Gras, *Comptes Rendus Hebdomadaires Des Séances de L'Académie Des Sciences* 180, 1485.

Desiraju, GR & Steiner, T (2000). *The Weak Hydrogen Bond*; International Union of Crystallography, Oxford Science Publication: Oxford, U.K.

Dickinson, RG & Raymond, AL (1923). The Crystal Structure of Hexamethylene-Tetramine, *J. Am. Chem. Soc.*, 45, 22. doi:10.1021/ja01654a003

Fitjer, L; Gerke, R; Weiser, J; Bunkoczi, G & Debreczeni, JE (2003). Helical Primary Structures of Four-membered Rings: (M)-trispiro[3.0.0.3.2.2]tridecane, *Tetrahedron*, 59, 4443.

Fuchter, MJ; Weimar, M; Yang, X; Judge, DK & White, AJP (2012). An Unusual Oxidative Rearrangement of [7]-Helicene, *Tetrahedron Lett.* 53, 1108-1111. doi:10.1016/j.tetlet.2011.12.082

Garcia, MH; Florindo, FP; Piedade, MFM; Maiorana, S & Licandro, E (2009). New Organometallic Ru(II) and Fe(II) Complexes with Tetrathia-[7]-helicene Derivative Ligands, *Polyhedron*, 28, 621.

Gilli, G & Gilli, P (2000). Towards an Unified Hydrogen-Bond Theory, *J. Mol. Struc.*, 552, 1.

Gilli, P; Bertolasi, V; Ferreti, V & Gilli, G (1994). Covalent Nature of the Strong Homonuclear Hydrogen Bond. Study of the O–H·····O System by Crystal Structure Correlation Methods, *J. Am. Chem. Soc.*, 116, 909.

Gilli, P; Bertolasi, V; Ferretti, V & Gilli, G (2000). Evidence for Intramolecular N-H·····O Resonance-Assisted Hydrogen Bonding in β-Enaminones and Related Heterodienes. A

Combined Crystal-Structural, IR and NMR Spectroscopic, and Quantum-Mechanical Investigation, *J. Am. Chem. Soc.*, 122, 10405-10417.

Gilli, P; Bertolasi, V; Pretto, L; Ferretti, V & Gilli, G (2004). Covalent versus Electrostatic Nature of the Strong Hydrogen Bond: Discrimination among Single, Double, and Asymmetric Single-Well Hydrogen Bonds by Variable-Temperature X-ray Crystallographic Methods in *β*-Diketone Enol RAHB Systems, *J. Am. Chem. Soc.*, 126, 3845-3855.

Golič, L; Hadži, D & Lazarini, F (1971). Crystal and Molecular Structure of the Hydrogen-bonded Adduct of Pyridine *N*-oxide with Trichloroacetic Acid, *J. Chem. Soc. D: Chem. Commun.*, 860a. doi:10.1039/C2971000860a

Groen, MB; Schadenberg, H & Wynberg, H (1971). Synthesis and Resolution of Some Heterohelicenes, *J. Org. Chem.* 36, 2797, and references therein.

Gulevskaya, AV; Serduke, OV; Pozharskii, AF & Besedin, DV (2003). 6,8-Dimethylpyrimido[4,5-*c*]pyridazine-5,7(6*H*,8*H*)-dione: New Heterocyclizations Based on (S_N^H)-Methodology. Unexpected Formation of the First iso-π-Electronic Analogue of the Still Unknown Dibenzo[*a*,*o*]pycene, *Tetrahedron*, 59, 7669-7679.

Guo, Z-Q; Chen, W-Q & Duan, X-M (2011). Seven-Membered Ring Excited-state Intramolecular Proton-Transfer in 2-Benzamido-3-(pyridin-2-yl)acrylic Acid, *Dyes and Pigments*, 92, 619-625.

Hamilton, GA (1971). In *Progress in Bioorganic Chemistry*, vol. 1, (Eds: Kaiser, ET; Kezdy, FJ), Wiley: New York, p 83.

Hosseini, Y; Rastgar, S; Heren, Z; Büyükgüngör, O & Noroozi Pesyan, N (2011). One-pot New Barbituric Acid Derivatives Derived from the Reaction of Barbituric Acids with BrCN and Ketones, *J. Chin. Chem. Soc.*, 58, 309.

Hussain, A; Hameed, S & Stoeckli-Evans, H (2009). 1-(4-Chlorophenylsulfonyl)-5-(4-fluorophenyl)-5-methylimidazolidine-2,4-dione, Acta Cryst., E65, o858–o859 and related references herein.

Hussain, A; Hameed, S & Stoeckli-Evans, H (2009). 1-(4-Methoxyphenylsulfonyl)-5-methyl-5-phenylimidazolidine-2,4-dione, Acta Cryst., E65, o1207–o1208 and related references herein.

Jacobsen, EN & Wu, MH (1999). *Comprehensive Asymmetric Catalysis Volume II*, ed. Jacobsen, EN; Pfaltz, A; Yamamoto, H, Springer-Verlag, Berlin-Heidleberg-New York, 1999, Chapt. 18.2, p. 649.

Jalilzadeh, M; Noroozi Pesyan, N; Rezaee, F; Rastgar, S; Hosseini, Y & Şahin, E (2011). New One-pot Synthesis of Spiro[furo[2,3-*d*]pyrimidine-6,5′-pyrimidine]pentaones and Their Sulfur Analogues, *Mol. Divers.*, 15, 721.

Jeffery, GA & Saenger, W (1991). *Hydrogen Bonding in Biological Structures*, Springer-Verlag, Berlin, Germany.

Jeffrey, GA & Saenger, W (1991). *Hydrogen Bonding in Biological Structures*, Springer-Verlag, Berlin, Chapt. 8.

Jeong, T-S; Kim, KS; Kim, J-R; Cho, K-H; Lee, S & Lee,WS (2004). Novel 3,5-Diaryl Pyrazolines and Pyrazole as Low-density Lipoprotein (LDL) Oxidation Inhibitor, *Bioorg. Med. Chem. Lett.*, 14, 2719-2723.

Johansson, MP & Patzschke, M (2009). Fixing the Chirality and Trapping the Transition State of Helicene with Atomic Metal Glue, *Chem. Eur. J.* 15, 13210.

Kashif, MK; Rauf, MK; Bolte, M & Hameed, S (2009). 3-(4-Chlorophenylsulfonyl)-8-methyl-1,3-diazaspiro[4.5]decane-2,4-dione, *Acta Cryst.*, E65, o1893.

Kashif, MK; Rauf, MK; Bolte, M & Hameed, S (2009).3-(4-Bromophenylsulfonyl)-8-methyl-1,3-diazaspiro[4.5]decane-2,4-dione, *Acta Cryst.*, E65, o1892.

Kato, S & Dryhurst, G (1975). Electrochemical Oxidation of Barbituric Acids at Low pH in the Presence of Chloride Ion, *J. Electroanal. Chem.* 62, 415-431.

Kato, S; Poling, M; van der Helm, D & Dryhurst, G (1974). Electrochemical Synthesis and Structure of a New Cyclic Barbiturate, *J. Am. Chem. Soc.* 96, 5255-5257.

Katritzky, AR & Rees, CW (eds.) (1997) Comprehensive Heterocyclic Chemistry, vol. 7. Pergamon Press, Oxford.

Katz, TJ & Pesti, J (1982). Synthesis of a Helical Ferrocene, *J. Am. Chem. Soc.* 104, 346.

Katz, TJ (2000). Syntheses of Functionalized and Aggregating Helical Conjugated Molecules, *Angew. Chem. Int. Ed.* 39, 1921.

Kiowski, W; Erne, P; Linder, L; Bühler, FR (1990). Arterial Vasodilator Effects of the Dihydropyridine Calcium Antagonist Amlodipine Alone and in Combination with Verapamil in Systemic Hypertension, *Am. J. Cardiol.*, 66,1469-1472.

Kotha, S; Deb, AC & Kumar, RV (2005). Spiro-annulation of Barbituric Acid Derivatives and Its Analogs By Ring-Closing Metathesis Reaction, *Bioorg. Med. Chem. Lett.*, 15, 1039.

Kumar, BCSA; Swamy, SN; Sugahara, K & Rangappa, KS (2009). Anti-tumor and Anti-angiogenic Activity of Novel Hydantoin Derivatives: Inhibition of VEGF Secretion in Liver Metastatic Osteosarcoma Cells, *Bioorg. Med. Chem.*, 17, 4928-4934.

Larsen, J; Dolbecq, A & Bechgaard, K (1996). Thiaheterohelicenes. 3. Donor Properties of a Series of Benzene-Capped Thiaheterohelicenes. Structure of a Tetrathianonahelicene and its TCNQ Salt, *Acta Chem. Scand.* 50, 83.

Liberko, CA; Miller, LL; Katz, TJ & Liu, L (1993). The Electronic Structure of Helicene-Bisquinone Anion Radicals, *J. Am. Chem. Soc.* 115, 2478.

Liu, L; Yang, B; Katz, TJ; Poindexter, MK (1991). Improved Methodology for Photocyclization Reactions, *J. Org. Chem.*, 56, 3769-3775.

Low, JN; Ferguson, G; Cobo, J; Nogueras, M; Cruz, S; Quirogae, J & Glidewell, C (2004). Three Hexahydropyridopyrimidine-spiro-cyclohexanetriones: Supra-molecular Structures Generated by O–H···O, N–H···O, C–H···O and C–H···π Hydrogen Bonds, and $\pi - \pi$ Stacking Interactions, *Acta Cryst.*, C60, o438-o443.

Madsen, GKH; Wilson, C; Nymand, TM; McIntyre, GJ & Larsen, FK (1999). The Structure of Nitromalonamide: A Combined Neutron-Diffraction and Computational Study of a Very Short Hydrogen Bond, *J. Phys. Chem. A*, 103, 8684-8690.

Maiorana, S; Papagni, A; Licandro, E; Annunziata, R; Paravidino, P; Perdicchia, D; Giannini, C; Bencini, M; Clays, K & Persoons, A (2003). A Convenient Procedure for the Synthesis of Tetrathia-[7]-helicene and the Selective Functionalisation of Terminal Thiophene Ring, *Tetrahedron* 59, 6481–648.

Martín, N; Guldi, DM & Sánchez, L (2005). Hydrogen-Bonding Motifs in Fullerene Chemistry, *Angew. Chem. Int. Ed.*, 44, 5374.

Martin, RH (1974). Die Helicene, *Angew. Chem.* 86, 727.

McGillivray, LR & Atwood, JL (1997). A Chiral Spherical Molecular Assembly Held Together By 60 Hydrogen Bonds, *Nature*, 389, 469.

McKinlay, RM; Thallapally, PK; Cave, GWV & Atwood, JL (2005). Hydrogen-Bonded Supramolecular Assemblies as Robust Templates in the Synthesis of Large Metal-Coordinated Capsules, *Angew. Chem. Int. Ed.* 44, 5733-5736.

Miyasaka, M; Rajca, A; Pink, M & Rajca, S (2005). Cross-Conjugated Oligothiophenes Derived from the $(C_2S)_n$ Helix: Asymmetric Synthesis and Structure of Carbon-Sulfur [11]-Helicene, *J. Am. Chem. Soc.* 127, 13806.

Müller, A (1923). The X-ray Investigation of Fatty Acids, *J. Chem. Soc. (London)*, 123, 2043.

Müller, A (1928). X-ray Investigation of Long Chain Compounds (n-Hydrocarbons), *Proc. R. Soc. Lond.* A, 120, 437-459. doi:10.1098/rspa.1928.0158

Müller, A (1929). The Connection between the Zig-Zag Structure of the Hydrocarbon Chain and the Alternation in the Properties of Odd and Even Numbered Chain Compounds, *Proc. R. Soc. Lond.* A, 124, 317-321. Bibcode 1929RSPSA.124..317M. doi:10.1098/rspa.1929.0117.

Nakagawa, H; Obata, A; Yamada, K & Kawazura, H (1985). Crystal and Molecular Structures of Tetrathia[7]-heterohelicene: Racemate and Enantiomer, *J. Chem. Soc., Perkin Trans. 2*, 1899-1903. doi:10.1039/P29850001899

Nakano, K; Oyama, H; Nishimura, Y; Nakasako, S & Nozaki, K (2012). λ^5-Phospha[7]helicenes: Synthesis, Properties, and Columnar Aggregation with One-Way Chirality, *Angew. Chem.*, 124, 719.

Naya, SI; Miyama, H; Yasu, K; Takayasu, T & Nitta, M (2003). Novel Synthesis and Properties of 7,9-Dimethylcyclohepta[b]pyrimido[5,4-*d*]furan-8(7*H*),10(9*H*)-dionylium Tetrafluoroborate: Autorecycling Oxidation of Some Alcohols Under Photo-irradiation, *Tetrahedron*, 59, 1811.

Nelson, JH (2002). *Nuclear Magnetic Resonance Spectroscopy*, Prentice Hall: New Jersey, pp 160, Chapt. 6.

Newman, MS & Chen, CH (1972). The Resolution and Absolute Configuration of 7-Methylhexahelicene, *J. Org. Chem.* 37, 1312.

Newman, MS & Lednicer, D (1956). The Synthesis and Resolution of Hexahelkenel, *J. Am. Chem. Soc.* 78, 4765.

Newman, MS; Darlak, RS & Tsai, L (1967). Optical Properties of Hexahelicene, *J. Am. Chem. Soc.* 89, 6191.

Newman, MS; Lutz, WB & Lednicer, D (1955). A New Reagent for Resolution by Complex Formation: The Resolution of Phenanthro[3,4-*c*]phenanthrene, *J. Am. Chem. Soc.* 77, 3420.

Nishio, M (2005). CH/π Hydrogen Bonds in Organic Reactions, *Tetrahedron*, 61, 6923-6950.

Noroozi Pesyan, N (2006). A New and Simple Method for the Specification of Absolute Configuration of Allenes, Spiranes, Alkylidenecycloalkanes, Helicenes and Other Organic Complex Systems, *Chem. Educ. J. (CEJ)*, 9(1), (Serial No. 16), http://www.juen.ac.jp/scien/cssj/cejrnlE.html.

Noroozi Pesyan, N (2010). Crystal Structure of 1,9-Dimethyl-4,5-dihydro-6H-pyrido[3',2':4,5]thieno[2,3-f]pyrrolo[1,2-a][1,4]diazepin-6-one, *J. Struct. Chem.* 51, 991-995.

Noroozi Pesyan, N; Rastgar, S & Hosseini, Y (2009). 1,1′,3,3′,5,5′-Hexamethylspiro[furo-[2,3-*d*]pyrimidine-6(5*H*),5′-pyrimidine]-2,2′,4,4′,6′(1*H*,3*H*,1′*H*,3′*H*,5*H*)-pentaone, *Acta Cryst.* E65, o1444.

Noroozi-Pesyan, N (2011). Isotopic Effect on Tautomeric Behavior of 5-(2,6-Disubstituted-aryloxy)-tetrazoles, *Magn. Reson. Chem.*, 49, 592.

Nuckolls, C; Katz, TJ & Castellanos, L (1996). Aggregation of Conjugated Helical Molecules, *J. Am. Chem. Soc.* 118, 3767.

Nuckolls, C; Katz, TJ; Verbiest, T; Van Elshocht, S; Kuball, H-G; Kiesewalter, S; Lovinger, AJ & Persoons, A (1998). Circular Dichroism and UV-Visible Absorption Spectra of the Langmuir-Blodgett Films of an Aggregating Helicene, *J. Am. Chem. Soc.* 120, 8656.

Olovsson, I; Ptasiewicz-Bak, H; Gustafsson, T & Majerz, I (2001). Asymmetric Hydrogen Bonds in Centrosymmetric Environment: Neutron Study of Very Short Hydrogen Bonds in Potassium Hydrogen Dichloromaleate, *Acta Cryst.* B57, 311

Piper, SH (1929). Some Examples of Information Obtainable from the long Spacings of Fatty Acids, *Trans. Faraday Soc.* 25, 348-351. doi:10.1039/tf9292500348

Poling, M & van der Helm, D (1976). 5,6-Dihydro-1,3-dimethyl-5,6-bis[1',3'-dimethyl-2',4',6'-trioxopyrimid(5,5')yl]furo[2,3-*d*]uracil, *Acta Crystallogr., Sect. B: Struct. Sci.* 32, 3349.

Pulacchini, S; Sibbons, KF; Shastri, K; Motevalli, M; Watkinson, M; Wan, H; Whiting, A & Lightfoot, AP (2003). Synthesis of *C*2-Symmetric Aza- and Azaoxa-macrocyclic Ligands Derived From (1*R*,2*R*)-1,2-Diaminocyclohexane and Their Applications in Catalysis, *Dalton Trans.*, 2043.

Rajca, A & Miyasaka, M In: Miller, TJJ; Bunz, UHF (Eds.) (2007). *Functional Organic Materials. Syntheses, Strategies, and Applications*, Wiley-VCH,Weinheim, p. 547.

Rajca, A; Miyasaka, M; Pink, M; Wang, H & Rajca, S (2004). Helically Annelated and Cross-Conjugated Oligothiophenes: Asymmetric Synthesis, Resolution, and Characterization of a Carbon-Sulfur [7]-Helicene, *J. Am. Chem. Soc.* 126, 15211.

Rimaz, M; Khalafy, J; Noroozi Pesyan, N & Prager, RH (2010). A Simple One-Pot, Three Component Synthesis of 3-Arylpyrimido[4,5-*c*]pyridazine-5,7(6*H*,8*H*)-diones and their Sulfur Analogues as Potential Monoamine, Oxidase Inhibitors, *Aust. J. Chem.*, 63, 507.

Rimaz, M; Noroozi Pesyan, N & Khalafy, J (2010). Tautomerism and Isotopic Multiplets in the ^{13}C NMR Spectra of Partially Deuterated 3-Arylpyrimido[4,5-*c*]pyridazine-5,7(6*H*,8*H*)-diones and Their Sulfur Analogs – Evidence for Elucidation of the Structure Backbone and Tautomeric Forms, *Magn. Reson. Chem.*, 48, 276.

Robertson, JM (1936). An X-ray Study of the Phthalocyanines, Part II, *J. Chem. Soc.*, 1195.

Sadarangani, IR; Bhatia, S; Amarante, D; Lengyel, I & Stephani, RA (2012). Synthesis, Resolution and Anticonvulsant Activity of Chiral *N*-1′-ethyl, *N*-3′-(1-phenylethyl)-(*R*,*S*)-2′*H*,3*H*,5′*H*-spiro-(2-benzofuran-1,4′-imidazolidine)-2′,3,5′-trione Diastereomers, *Bioorg. Med. Chem. Lett.*, 22, 2507-2509.

Saville, WB & Shearer, G (1925). An X-ray Investigation of Saturated Aliphatic Ketones, *J. Chem. Soc. (London)* 127, 591.

Schmuck, C (2003). Molecules with Helical Structure: How To Build a Molecular Spiral Staircase, *Angew. Chem. Int. Ed.* 42, 2448.

Severa, L; Adriaenssens, L; Vávra, J; Šaman, D; Císařová, I; Fiedler, P & Teplý, F (2010). Highly Modular Assembly of Cationic Helical Scaffolds: Rapid Synthesis of Diverse Helquats via Differential Quaternization, *Tetrahedron*, 66, 3537.

Sheldrick, GM (1997). *SHELXL97*, University of Göttingen, Göttingen, Germany.

Si, HZ; Wang, T; Zhang, KJ; Hu, ZD; Fan, BT (2006). QSAR Study of 1,4-Dihydropyridine Calcium Channel Antagonists-Based on Gene Expression Programming, *Bioorg. Med. Chem.*, 14, 4834-4841.

Smith, BM & March, J (2001). *Advanced Organic Chemistry, Reactions, Mechanism, and structure*, 5th ed., John Wiley & Sons, New York, p. 134.

Steiner, T (2002). The Hydrogen Bond in the Solid State, *Angew. Chem. Int. Ed.*, 41, 48.

Stoe & Cie, (2002). *X-AREA*. Stoe & Cie, Darmstadt, Germany.

Sudhakar, A & Katz, TJ (1986). Asymmetric Synthesis of Helical Metallocenes, *J. Am. Chem. Soc.* 108, 179.

Sudhakar, A & Katz, TJ (1986). Directive Effect of Bromine on Stilbene Photocyclizations. an Improved Synthesis of [7]-helicene, *Tetrahedron Lett.*, 27, 2231.

Taylor, R & Kennard, O (1982). Crystallographic Evidence for the Existence of C-H···O, C-H···N, and C-H···Cl Hydrogen Bonds, *J. Am. Chem. Soc.*, 104, 5063.

Trillat, JJ (1926). Rayons X et Composeés Organiques à Longe Chaine. Recherches Spectrographiques Sue Leurs Structures et Leurs Orientations, *Annales de physique* 6, 5.

Urbano, A (2003). Recent Developments in the Synthesis of Helicene-Like Molecules, *Angew. Chem. Int. Ed.* 42, 3986.

Vishweshwar, P; Babu, NJ; Nangia, A; Mason, SA; Puschmann, H; Mondal, R & Howard, JAK (2004). Variable Temperature Neutron Diffraction Analysis of a Very Short O-H···O Hydrogen Bond in 2,3,5,6-Pyrazinetetracarboxylic Acid Dihydrate: Synthon-Assisted Short O_{acid}-H···O_{water} Hydrogen Bonds in a Multicenter Array, *J. Phys. Chem. A*, 108, 9406-9416.

Wang, X-B; Woo, HK; Kiran, B & Wang, L-S (2005). Observation of Weak C–H···O Hydrogen Bonding to Unactivated Alkanes, *Angew. Chem. Int. Ed.* 44, 4968-4972.

Watkin, DJ; Müller, M; Blèriot, Y; Simonec, MI & Fleet, GWJ (2004). (2*S*,3*R*,4*R*,5*S*)-3,4-*O*-Isopropylidene-2-methyl-1-oxa-6,9-diazaspiro[4.5]decane-7,10-dione, *Acta Cryst.*, E60, o1820-o1822.

Wilson, CC (2000). *Single Crystal Neutron Diffraction From Molecular Materials* (1st edn), vol. 2, World Scientific Publishing Co. Pte. Ltd.: Singapore, Chapts. 4, 5 and 7.

Wynberg, H (1971). Some Observations on the Chemical, Photochemical, and Spectral Properties of Thiophenes, *Acc. Chem. Res.* 4, 65-71.

Yamada, K; Ogashiwa, S; Tanaka, H; Nakagawa, H & Kawazura, H (1981). [7],[9],[11],[13] and [15] Heterohelicenes Annelated With Alternant Thiophene and Benzene Rings. Syntheses and NMR Studies, *Chem. Lett*., 343.

Yang, W-B; Lu, C-Z; Wu, C-D; Wu, D-M; Lu, S-F & Zhuang, H-H, (2003). Synthesis and Crystal Structure of Bis(barbiturato)triwater Complex of Copper(II), *Chinese J. Struct. Chem.* 22, 270.

Yoshida, N; Ito, N & Ichikawa, K (1997). Formation of a Three-Dimensional Hydrogen-Bonding Network by Self-assembly of the CuII Complex of a Semi-bidentate Schiff Base, *J. Chem. Soc., Perkin Trans. 2*, 2387.